

**ISTANBUL TECHNICAL UNIVERSITY ★ EURASIA INSTITUTE OF EARTH
SCIENCES**

**DISTRIBUTION OF QUATERNARY DEFORMATION ALONG
THE COASTS OF CYPRUS, INFERENCES FROM MARINE TERRACES**



M.Sc. THESIS

Cevza D. ALTINBAŞ

Department of Solid Earth Sciences

Geodynamics Programme

MAY 2018

**ISTANBUL TECHNICAL UNIVERSITY ★ EURASIA INSTITUTE OF EARTH
SCIENCES**

**DISTRIBUTION OF QUATERNARY DEFORMATION ALONG
THE COASTS OF CYPRUS, INFERENCES FROM MARINE TERRACES**



M.Sc. THESIS

**Cevza D. ALTINBAŞ
(602141005)**

Department of Solid Earth Sciences

Geodynamics Programme

Thesis Advisor: Assoc.Prof. Cengiz YILDIRIM

MAY 2018

İSTANBUL TEKNİK ÜNİVERSİTESİ ★ AVRASYA YER BİLİMLERİ
ENSTİTÜSÜ

KIBRIS KIYILARINDA KUVATERNER DEFORMASYONUN DAĞILIMI
DENİZEL TERASLARDAN ÇIKARIMLAR

YÜKSEK LİSANS TEZİ

Cevza D. ALTINBAŞ
(602141005)

Katı Yer Bilimleri Anabilim Dalı

Jeodinamik Programı

Tez Danışmanı: Doç. Dr. Cengiz YILDIRIM

MAYIS 2018

Cevza D. Altınbaş, a M.Sc. student of ITU Eurasia Institute of Earth Sciences 602141005, successfully defended the thesis entitled “Distribution of Quaternary Deformation Along the Coasts of Cyprus, Inferences from Marine Terraces”, which she prepared after fulfilling the requirements specified in the associated legislations, before the jury whose signatures are below.

Thesis Advisor : **Assoc.Prof. Cengiz YILDIRIM**
İstanbul Technical University

Jury Members : **Assoc.Prof. Cengiz YILDIRIM**
İstanbul Technical University

Prof. Dr. Okan TÜYSÜZ
İstanbul Technical University

Assist.Prof. Tolga GÖRÜM
İstanbul University

Date of Submission : 26 April 2018

Date of Defense : 08 May 2018





To my Grandma,



FOREWORD

I would like to thank Okan Tüysüz, Cengiz Yıldırım and Daniel Melnick who gave me a new vision in the field work we have done in Cyprus and in the studies that we have done in the future. I would also like to thank Orkan Özcan, who has supported me throughout my undergraduate studies and thank to Julius Jara for all technical support.

February 2018

Cevza D. ALTINBAŞ



TABLE OF CONTENTS

	<u>Page</u>
FOREWORD	ix
TABLE OF CONTENTS	xi
ABBREVIATIONS	xiii
LIST OF TABLES	xv
LIST OF FIGURES	xvii
SUMMARY	xix
ÖZET	xxi
1. INTRODUCTION	1
2. REGIONAL SETTINGS	3
3. DATA AND METHODS	9
4. RESULTS	13
4.1 Marine Terraces in Northern Cyprus	13
4.1.1 Cape Karpaz	13
4.1.2 Dipkarpaz	15
4.1.3 Yeni Erenköy	17
4.1.4 Tatlısu.....	19
4.1.5 Kyrenia.....	21
4.1.6 Akdeniz	22
4.2 Marine Terraces in Southern Cyprus.....	25
4.2.1 Yeronisos	25
4.2.2 Paphos	28
5. DISCUSSION	31
5.1 Implications For Rate And Deformation Pattern In The Northern Cyprus.....	31
5.2 Implications For Rate And Deformation Pattern In The Southern Cyprus.....	32
5.3 Distribution Of Quaternary Deformation On The Cyprus Island	34
6. CONCLUSION	37
REFERENCES	39
CURRICULUM VITAE	47



ABBREVIATIONS

a.s.l	: Above Sea Level
DEM	: Digital Elevation Model
GIS	: Geographic Information System
MIS	: Marine Isotope Stage





LIST OF TABLES

	<u>Page</u>
Table 2.1 : List of most important historical earthquakes from Zomeni (2012).....	8
Table 3.1 : MIS stands for marine isotope stages from Zomeni, (2012).....	12
Table 5.1 : Temporal Marine Isotope Stages, total displacements and uplift rates to highest elevation of terraces.	35
Table 5.2 : Temporal Marine Isotope Stages, total displacements and uplift rates to MIS 5 level terraces.	35





LIST OF FIGURES

	<u>Page</u>
Figure 2.1 : Simplified tectonic map of the eastern Mediterranean Region (Topography and Bathymetry NOAA GLOBE 1Km, GMRT Image Version 3.4 data compiled from GeoMapApp).	3
Figure 2.2 : Geological Map of Cyprus	4
Figure 2.3 : Geological cross-sections across the Kyrenia thrust belt and Mesaoria Basin from Calon, 2005	6
Figure 2.4 : The distribution of modern earthquakes and focal mechanism solutions with a magnitude greater than $M_w > 4, 5$ in the region. The data compiled by GeoMapApp.	7
Figure 3.1 : The TerraceM interface	9
Figure 3.2 : Comparison between the reconstruction of the past global mean sea level and paleo-climatic, paleo-environmental and archaeological data for the Mediterranean Sea	10
Figure 3.3 : Relationship between sea-level variation and geomorphic record on uplifting coasts from Pedoja et Al. (2014).	11
Figure 4.1 : Marine terraces and shoreline angles of Cape Carpaz.	13
Figure 4.2 : TerraceM results of Cape Carpaz, shoreline angles on profiles.	14
Figure 4.3 : Marine terraces and shoreline angles of Dipkarpaz.	15
Figure 4.4 : TerraceM results of Cape Carpaz, shoreline angles on profiles.	16
Figure 4.5 : Marine terraces and shoreline angles of Yeni Erenköy.	17
Figure 4.6 : TerraceM results of Yeni Erenköy, shoreline angles on profiles. .	18
Figure 4.7 : Marine terraces and shoreline angles of Tatlısu.	19
Figure 4.8 : TerraceM results of Tatlısu, shoreline angles on profiles.	20
Figure 4.9 : Marine terraces and shoreline angles of Kyrenia.	21
Figure 4.10 : TerraceM results of Kyrenia, shoreline angles on profiles.	22
Figure 4.11 : Marine terraces and shoreline angles of Akdeniz.	23
Figure 4.12 : TerraceM results of Akdeniz, shoreline angles on profiles.	24
Figure 4.13 : Marine terraces and shoreline angles of Yeronisos.	25
Figure 4.14 : TerraceM results of Yeronisos, shoreline angles on profiles.	26
Figure 4.15 : TerraceM results of Yeronisos, Profile 3.	27
Figure 4.16 : Marine terraces and shoreline angles of Paphos.	28
Figure 4.17 : TerraceM results of Paphos.	29



DISTRIBUTION OF QUATERNARY DEFORMATION ALONG THE COAST OF CYPRUS INFERENCES FROM MARINE TERRACES

SUMMARY

Cyprus is located on the subduction zone between African and Eurasia Plates. The topography of the island is a result of distributed deformation associated with the subduction related processes in the south of the Eurasia Plate. Trodos and Kyrenia mountains are major morphotectonic units that integrally tied to plate boundary deformations. The presence of uplifted marine terraces is piece of evidence of subduction related active deformation in the part of the island. To understand rate and pattern of deformation, I conducted geomorphic mapping of marine terraces by ArcGIS and analyzing of paleo-cliffs by TerraceM Matlab based program. As a result of these analyzes I calculated the uplift rates with reference to MIS 5. Here will present morphotectonic implications from temporal and spatial distribution of marine terraces along the Cyprus.



KIBRIS KIYILARINDA KUVATERNER DEFORMASYONUN DAĞILIMI, DENİZEL TERASLARDAN ÇIKARIMLAR

ÖZET

Kıbrıs adası, Afrika ve Avrasya Plakaları arasındaki dalma-batma bölgesinde bulunmaktadır. Adanın topografyası Avrasya plakasının güneyindeki dalma-batma ile ilişkili deformasyonların bir sonucudur. Trodos ve Girne Dağları, plaka sınır deformasyonlarına bütün olarak bağlı büyük morfotektonik birimlerdir. Yükselen deniz teraslarının varlığı adanın bir bölümünde dalma-batmaya bağlı aktif deformasyonun bir parçasıdır. Deformasyonun hızını ve desenini anlamak için ArcGIS ile denizel terasların jeomorfik haritalamasını ve eski kıyı çizgisi yüksekliklerinin Matlab tabanlı bir program olan Terracem tarafından analiz edilmesi sağladım. Bu analizler sonucunda MIS 5'e göre yükselme hızlarını hesapladım. Burada, denizel terasların yükselme hızlarının zamansal ve mekansal dağılımının Kıbrıs'ın geneline olan morfotektonik etkileri sunulmuştur.



1. INTRODUCTION

Along coastal zones, uplifted marine terraces form tectonic strain markers that record the rates of crustal deformation (Bloom et al., 1974; Merritts and Bull, 1989; Pedoja et al., 2006; Bishop, 2007; Caputo et al., 2010; Melnick et al., 2012). Uplifted marine terraces in these environments are created by a combination of sea level changes and vertical crustal movements (Lajoie, 1986). The uplift rate of marine terraces can be analyzed with sum of coseismic and interseismic movements with respect to the position of the corresponding paleo sea-level during terrace formation (Lajoie, 1986). Coastal geomorphology often reflects regional patterns or even large-scale tectonic patterns (Pedoja et al., 2011).

The third largest Mediterranean island Cyprus is located on the subduction zone between African and Anatolian Plates. The subduction zone in which this boundary is represented is called Cyprus Arc (Fig.2.1). Cyprus and Hellenic Arc together form a “double arc” system (Veen, 2004). This subduction zone in the Eastern Mediterranean Sea is the include last remains of Neotethys. Subduction beneath the Cyprus Arc appears to have stopped because of Eratosthenes Seamount (Robertson, 1998).

This distinctive geographical location reveals various tectonic events and geomorphological elements like coastal morphological features; uplifted marine terraces, wave-cut notches and abrasion platforms. In this study, uplifted marine terraces on the coast of Cyprus island were analyzed.



2. REGIONAL SETTINGS

African Plate subducts beneath Aegean and Anatolian Plates along the Hellenic and Cyprus arcs, respectively (Fig.2.1). The rate of northward movement of the African Plate is 10 mm/yr. (Aksu et al. 2005). Cyprus Arc is located between Hellenic Arc in the west and Dead Sea Transform Fault in the east. By left lateral motion of Dead Sea Transform Fault the rate of the differential movement between Africa Plate and Arabian Microplate is ~15 mm/yr. (Barka, 1997).

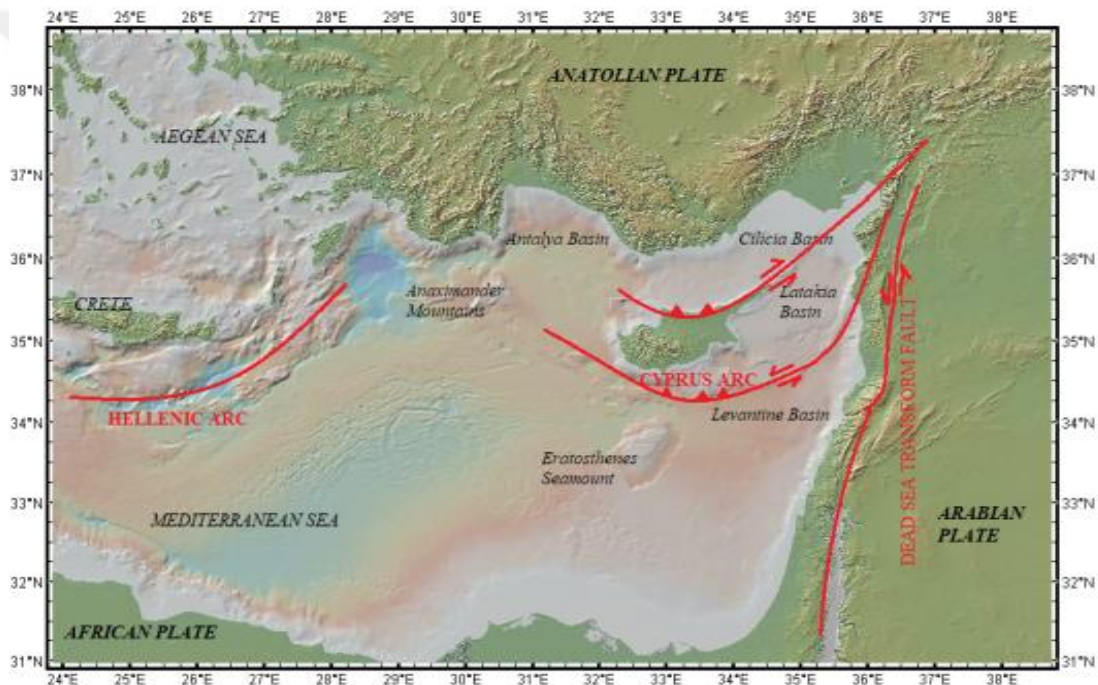


Figure 2.1 : Simplified tectonic map of the eastern Mediterranean Region (Topography and Bathymetry NOAA GLOBE 1Km, GMRT Image Version 3.4 data compiled from GeoMapApp).

East-west long axis of the island is 225 km and north-south short axis is 97 km. The Trodos and Kyrenia Mountains are the mountain ranges in the Island. The highest peak of the Trodos Mt. is 1,952 m a. s. l and the highest peak of the Kyrenia Mt. is 1,024 m above sea level. Mesaoria is the large depression between those two mountain ranges. Cyprus is divided into three major physical regions corresponding with the main geological divisions. They are:

- 1) The Trodos Mountains, in the south,

- 2) The Kyrenia Range along the northern coast, and
- 3) The Mesaoria Plain, stretches from the center (Dreghorn,1978).

The Trodos Mountains made up rocks from Upper Cretaceous. These rocks are oceanic rocks consist of ofiyolitic. Serpentinite and Harzburgite (Mantle Sequence), Dunite, Wehrlite, Pyroxenite, Gabbro and Plagiogranite (Plutonic Sequence), Diabase (Intrusive Sequence), Basal group, Lower Pillow Lavas and Upper Pillow Lavas (Volcanic Sequence) are concentricly form core of the Trodos mountain

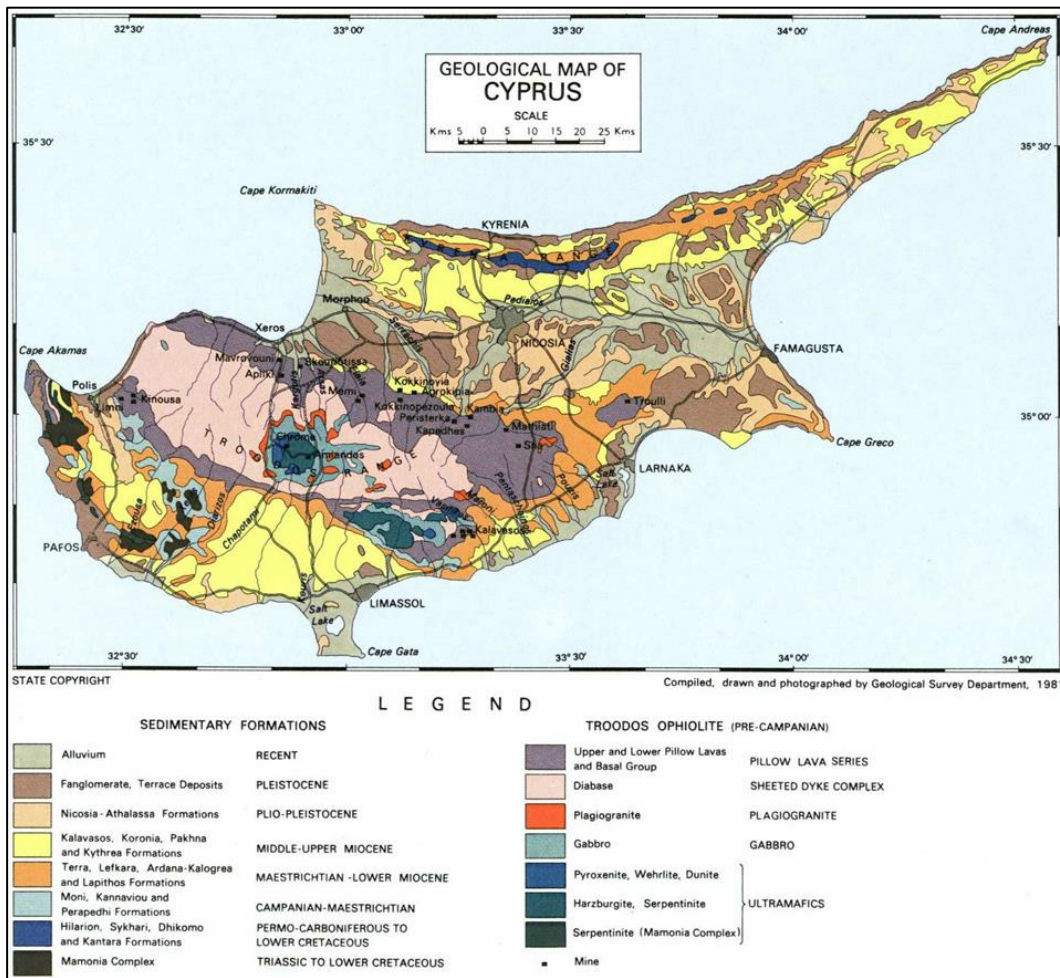


Figure 2.2 : Geological Map of Cyprus.

The Kyrenia range has complex assemblage rock units made up Permian to Quaternary. The Permian rocks are massive limestones and represented as Kantara Formation. The Lower Triassic to Lower Cretaceous rock formations are the allochthonous as Dhikomo, Sykhari and Hilarion Formations, which form the main carbonate masses of the Kyrenia Range. The Dhikomo Formation consists of deformed thinly bedded marbles in places thin micaceous with thin intercalations of

Phyllites. The Sykhari Formation is consist of mostly recrystallized and brecciated dolomitic limestones. The Hilarion Formation consists of recrystallized massive -or medium-to thick- bedded limestones, which were exposed to a low degree of metamorphism. The Upper Cretaceous to Quaternary formations are the Lapithos, Kalogrea-Ardana and Kythrea has younger autochthonous marine sediments. The Lapitos Formation is consist of Chalks, massive recrystallized white Limestone, recrystallized basal Breccia and Rhyolite blocks. The Kalogrea-Ardana Formation is consist of Grits, Greywackes and usually very coarse recrystallized basal Breccia. The Kythrea Formation has a youngest sediments is consist of Greywacke, Sandstone, siltstones and basal conglomerates (Fig.2.2).

Mesaoria depression is mainly made up sediments from Pliocene to Holocene and consist of Fanglomerate and Alluvium-Colluvium Formations. The contents of these formations are generally gravels, sand, silt and clay (Fig.2.2).

The Cyprus Arc is the major structure in the south of the island. The Florence Rise, the Anaximander Seamount and the Antalya Basin are the distinctive structures of the compression surrounding west of the Cyprus Arc (Fig.2.1). Eratosthenes and Hecataeus Seamounts are include of collisional features and they are distinctive structures in the south of the Cyprus arc. The Cilicia Basin is presently situated in a fore-arc setting, north of the Cyprus Arc (Aksu et al.2005). The Kyrenia Thrust Belt curves northward in the Cilicia Basin and forms a Misis-Kyrenia fault zone in this basin. Structural compaction in the Late Miocene formed imbricated faults (Fig.2.3) in the fore-arc region, especially in the Kyrenia Thrust Belt (Calon, 2005).

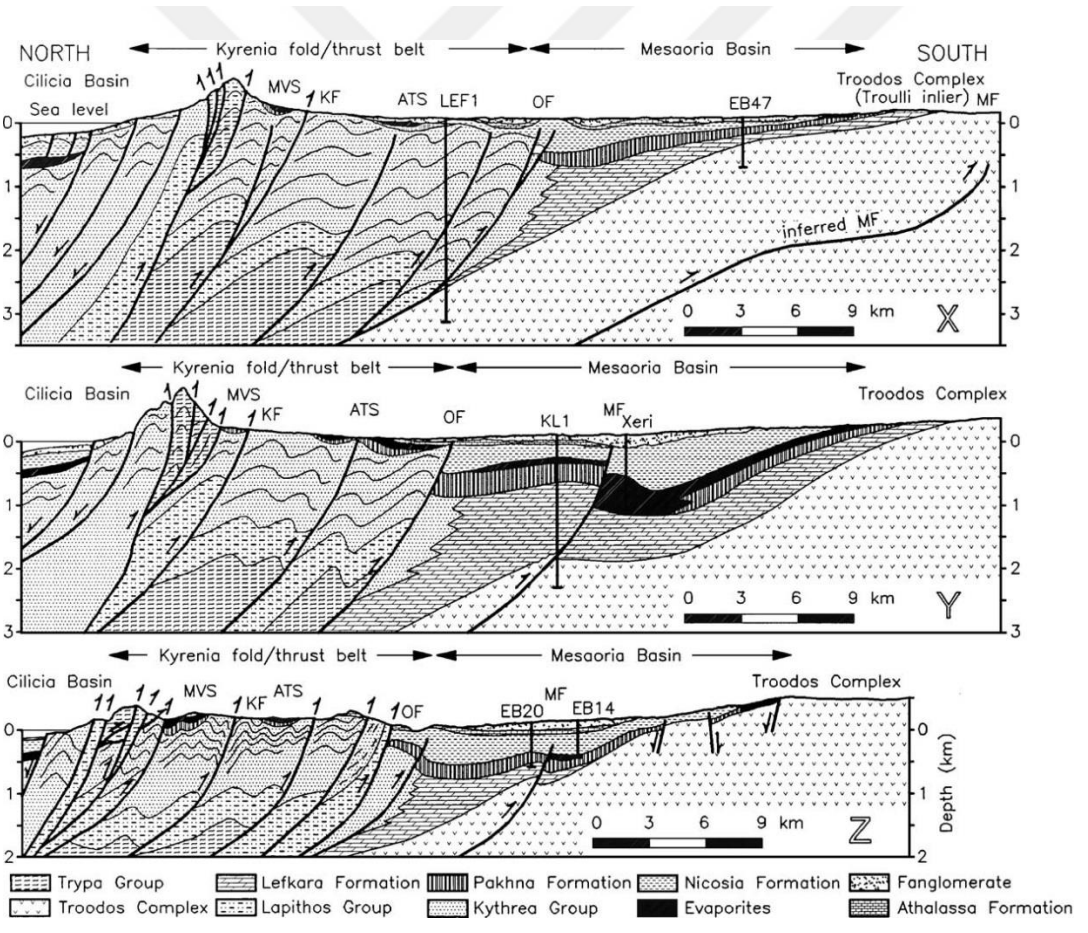
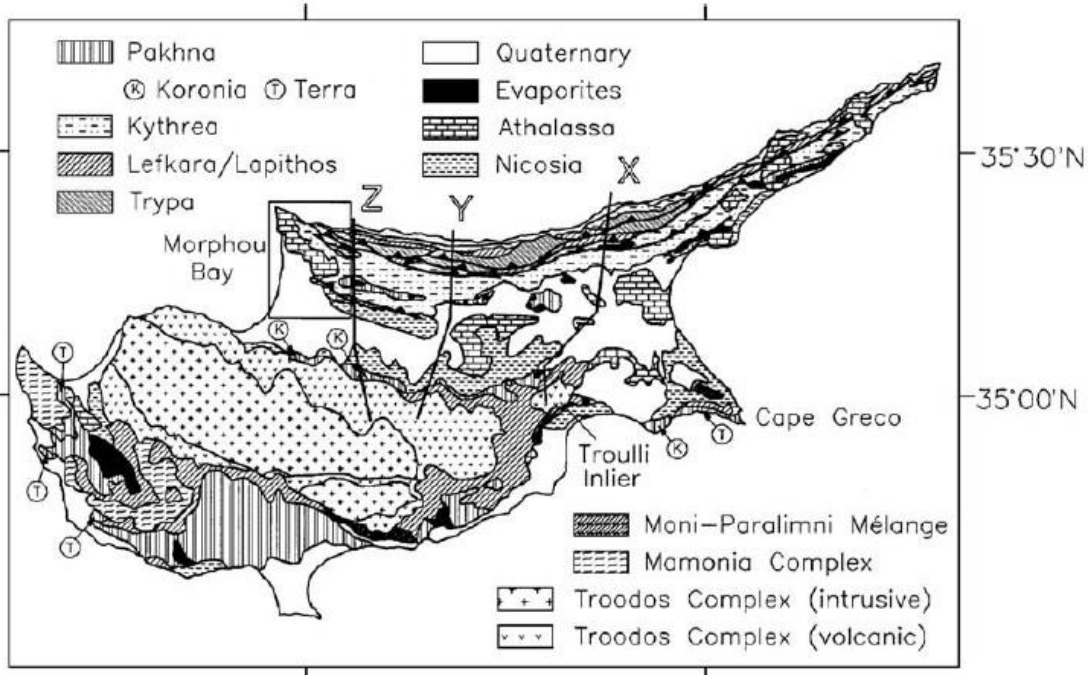


Figure 2.3 : Geological cross-sections across the Kyrenia thrust belt and Mesaoria Basin from Calon, 2005.

In the Kyrenia Thrust Belt Ovgos Fault is a major tectonic boundary in Cyprus. Ovgos Fault has a slightly curved, east-west trend and separates the Kyrenia Range to the north from the Mesaoria Plain succession to the south. Northern Cyprus is affected by the left lateral strike motion along the Ovgos Fault from the escape of Anatolia to the Hellenic subduction zone (McCay and Robertson, 2012).

The island of Cyprus and its surroundings have had major destructive earthquakes in the historical period (Table 2.1). Earthquakes recorded during the instrumental period are distributed along the Cyprus Arc in south of the island and with shallow-medium depth earthquakes offshore Paphos and that indicates Paphos Transform Fault. According to Papazachos (1999), the fault plane solutions of earthquakes show that Paphos Transform Fault forms a strike slip, with a thrust component, dextral fault. The subcrustal depth earthquakes are concentrated in the Antalya Basin and these earthquakes may indicate of subduction here. Although there are 11 earthquakes with a moment magnitude greater than 4,5 in the south of Cyprus and no earthquake in the north of the island where a moment magnitude solution can be generated (Fig.2.4).

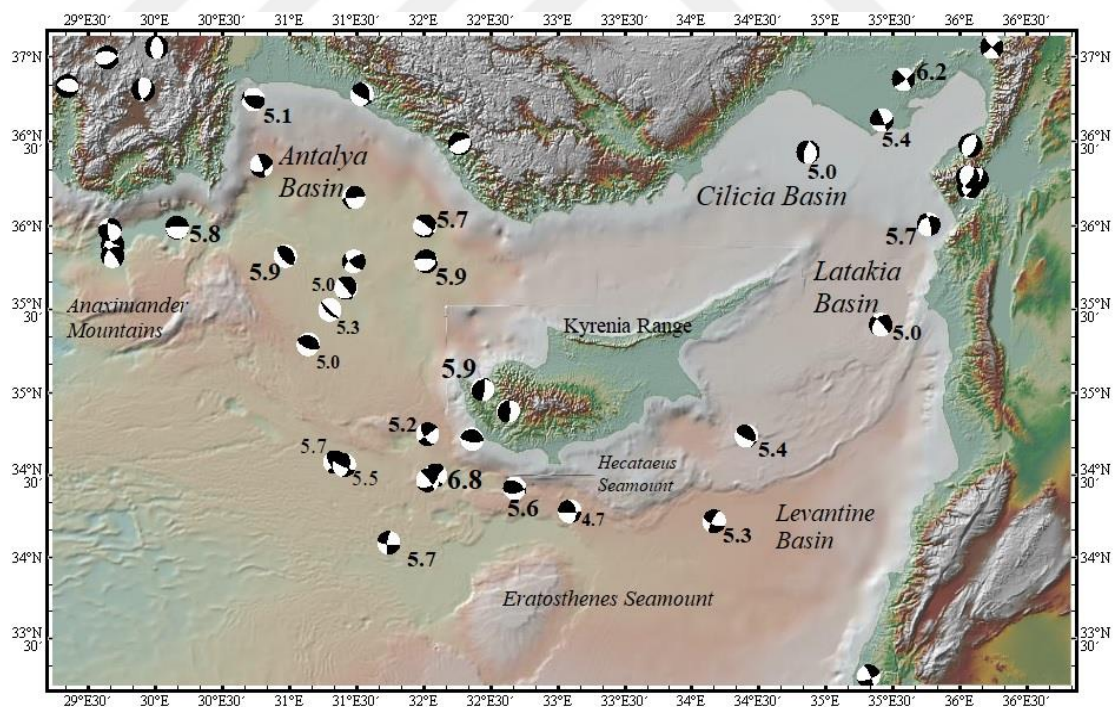


Figure 2.4 : The distribution of modern earthquakes and focal mechanism solutions with a magnitude greater than $M_w > 4, 5$ in the region. The data compiled by GeoMapApp.

Table 2.1 : List of most important historical earthquakes from Zomeni (2012).

BC	Year
Destructive earthquake in Paphos and Egypt	26
Destructive earthquake in Paphos and Kourion	15
AD	
Destructive earthquake in Paphos and Amathous	6
Most destructive earthquake and tsunami in Paphos, Salamis, Kition	76-77
Destructive earthquake in Salamis	332
Destructive earthquake and tsunami in Paphos	342
Destructive earthquake and tsunami in Crete	21 July 365
Destructive earthquake in Kourion and Akrotiri	367
Earthquake in Paphos and Salamis	394
Earthquake in Paphos area	19 May 1144
Earthquake in Paphos and NNE of Nea Paphos	1183
Earthquake in Cyprus and tsunami in Eastern Mediterranean	1202-3
Earthquake in Paphos and Lefkoşa	3 May 1481
Earthquake in Paphos	18 December 1481
Earthquake felt on the whole island	25 May 1491
Earthquake in Paphos district	Dec 1567
Destructive earthquake (6.3 Ms) in Paphos district with 63 dead, 200 wounded and 4000 homeless.	1953

3. DATA AND METHODS

In this study, 16 bit and 9235x7455 resolution, 30 m ALOS DEM (Digital Elevation Model) data was used. This DEM stretched and classified according to elevations. For this data, stretched type is 'Standard Deviation' (n value is 8) and classification type is 'Natural Breaks' (5 classes). And then with the geoprocessing tool 'surface' in ArcToolbox, was created a feature class of contours (isolines) of 10 meters intervals from a raster surface.

Based on DEM data and in-situ field observations (only for northern cyprus) I mapped marine terraces. Regions with Quaternary marine terraces in the north and south of the island were selected and exported in the global mapper program to save the determined regions in ascii format. The swath profiles were drawn with the editor toolbox on ArcGIS for each terrace in these regions for use in the TerraceM. TerraceM is a Matlab(R) for mapping marine and lacustrine terraces using high resolution topography. TerraceM has been designed by Julius Jara, Daniel Melnick and Manfred Strecker at the University of Potsdam, Germany. It is an open source programme (http://www2.udec.cl/~jujara/TerraceM/pivotx_latest) (Fig.3.1).

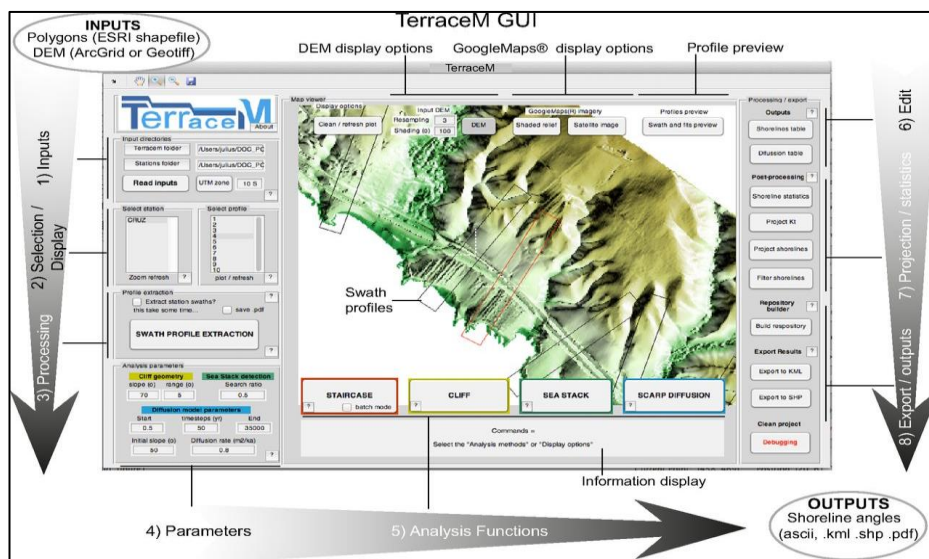


Figure 3.1 : The TerraceM interface.

The “Analytical Functions” are defined by four different functions. These are staircase, cliff, sea stack and scarp diffusion functions. Staircase and cliff analytic functions are used in this study. With cliff analysis, I found the shoreline angles for each marine terraces. A shoreline angle of a marine terrace is the ideal geomorphic data to calculate the relative elevation of past sea-level positions.

The Quaternary terraces, morphotectonic analyzes performed with the ArcGIS and TerraceM program, was mapped according to MIS stages. I used published age data to correlate marine terrace levels was dated Northern Cyprus sediments to the Pleistocene – Tyrrhenian stage and Pantazis (1967) dated the Kyrenia terrace to the Middle Pleistocene or the Tyrrhenian 2 stage, Ducloz (1968) dated the Kyrenia terrace deposits to MIS 5 (Galili et. Al,2015).

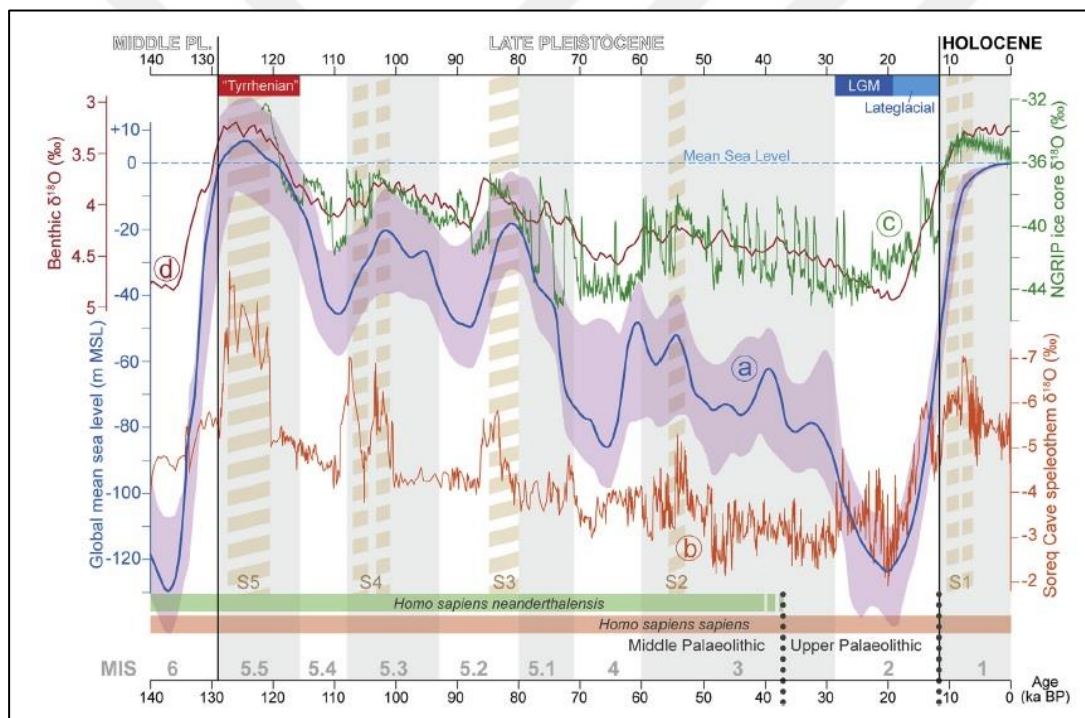


Figure 3.2 : Comparison between the reconstruction of the past global mean sea level and paleo-climatic, paleo-environmental and archaeological data for the Mediterranean Sea since 140 ka. **a)** Global mean sea-level curve with uncertainty indicated in light blue (Waelbroeck et al., 2002). As a paleo-climatic proxy for the SE Mediterranean region the $\delta^{18}O$ composition of the Soreq Cave speleothem **(b)** is plotted, while for the paleo-climate of the Northern Hemisphere, the $\delta^{18}O$ composition of NGRIP ice core **(c)** is represented (NGRIP members, 2004; Kindler et al., 2014). Grey and white rectangles indicate the MIS according to the LS16 $\delta^{18}O$ stacked benthic composition **(d)** (Lisiecki and Stern, 2016). Brown dashed shading indicates periods of sapropel deposition (Rohling et al., 2015). Figure and description from Benjamin, J. et al. (2017).ulti-line figure captions, it is important that all the lines of the caption are aligned.

Global sea-level changes in the last 2 million years that were caused by glaciation cycles (Fig.3.2), led to global falls in sea-level to as low as 130 m below the present level (Galili et al. 2015). In addition, information on older sea-level histories is certainly even more hypothetical (Fig.3.3), in spite of the current data of the global trend of sea level oscillation (Pedoja et Al. 2014). Marine terraces from tectonically uplifted regions provides information about past highest sea-level maximum. The most obvious marine terraces in the Mediterranean are formed at MIS 5 and indicates the last interglacial period.

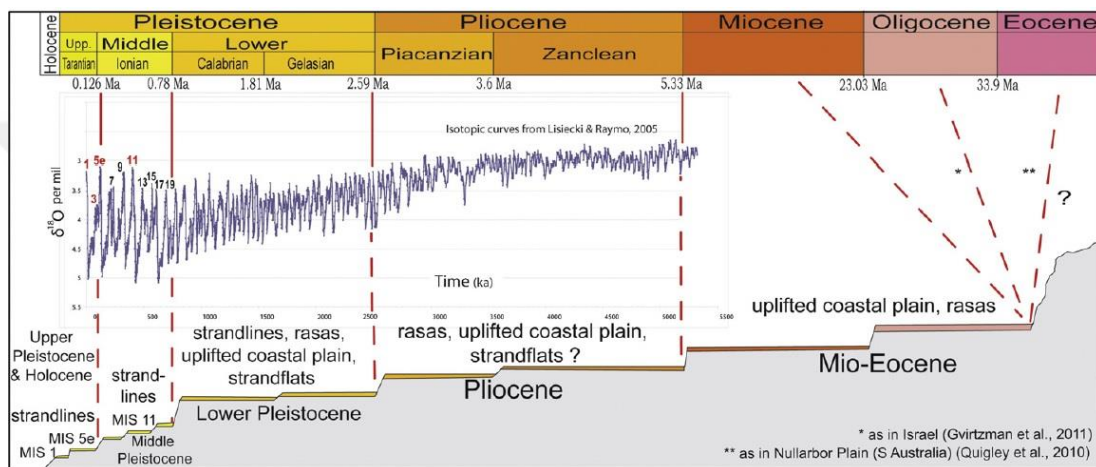


Figure 3.3 : Relationship between sea-level variation and geomorphic record on uplifting coasts from Pedoja et Al. (2014).

According to Zomeni and others, terraces at the highest elevation on the island of Cyprus are Pliocene age (Poole et al., 1990; Tsiolakis and Zomeni, 2008; Kinnaird, 2008).

Table 3.1 : MIS stands for marine isotope stages from Zomeni, (2012).

MIS	Peak of MIS (years BP)	Sea level relative to present m.s.l. (m)
1	0	0
2	18,000	-120
3	40,000	-62
4	65,000	-84
5a	81,000	-19 ± 5
5b	87,500	-48
5c	100,000	-20 ± 3
5d	110,000	-44
5e	124,000	+6 ± 3
6	134,000	-129
7	216,000	-3.5
8	250,000	-108
9	330,500	+5
10	344,000	-126
11	402,000	+6

Uplift rates of the coastal terraces (Table.3), the results of all swath profiles calculated shoreline angles. In this study, vertical displacement of marine terraces calculated by using the difference between the present terrace elevation (E) and the shoreline angle elevation (e) of the terrace with the highest MIS value. To calculate the uplift rate (U) of terrace, the vertical displacement divided by the MIS age (A) of the marine terrace (Lajoje, 1986):

$$U = (E - e) / A \quad (1)$$

4. RESULTS

4.1 Marine Terraces in Northern Cyprus

4.1.1 Cape Karpaz

The Cape Karpaz is located at the easternmost part of the island. Marine terraces are developed over the sand stones here. I employed two swath profiles that across well preserved cliffs of the paleo-shorelines. Accordingly, I identified 5 levels of paleo-shorelines up to 82 meters.

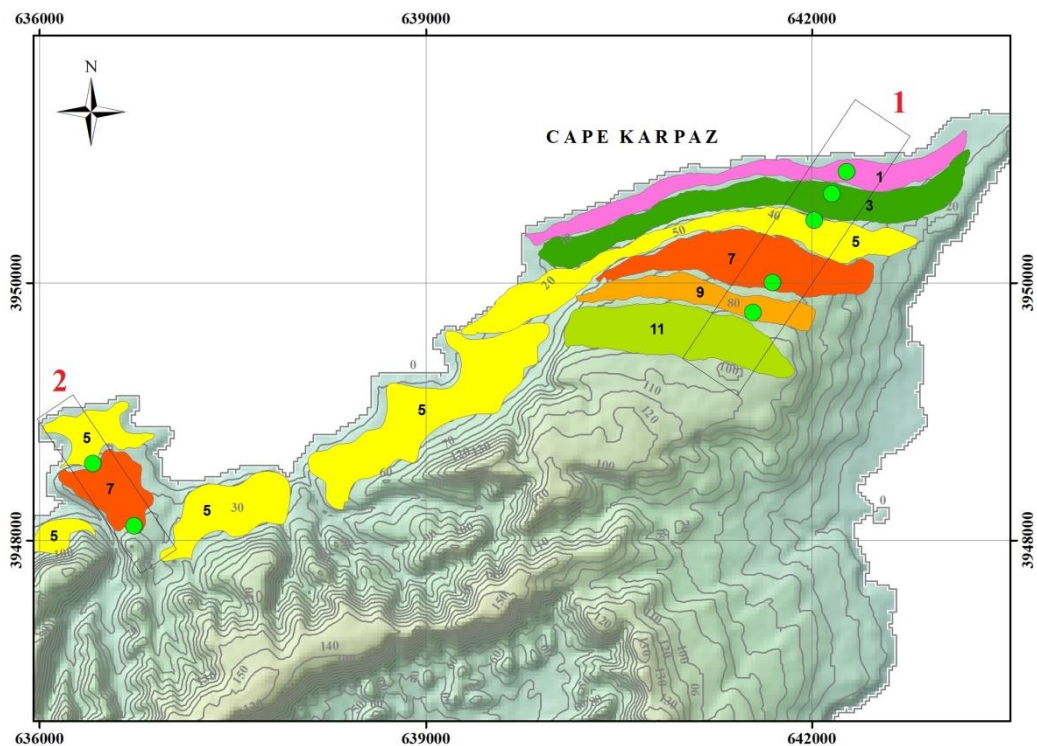


Figure 4.1 : Marine terraces and shoreline angles of Cape Carpaz.

In the first swath profile of Cape Karpaz, elevation values of six terrace surfaces and five shoreline angle values of these terraces are produced in Terracem. Although there are 6 levels determined by looking at the satellite images, there are five different terraces in DEM generated map (Fig.4.1). The shoreline angles were seen at (T1) 5.06 ± 0.85 m, (T2) 13.90 ± 0.97 m, (T3) 19.87 ± 2.39 m, (T4) 71.54 ± 0.80 m and (T5) 79.34 ± 1.10 meters above the sea level (Fig.4.2). Shoreline angles of terraces are shown in green dots. In the second swath profile, there are two terrace surfaces with elevations at (T1) $13,65 \pm 0.20$ m and (T2) $32,09 \pm 1.15$ meters were determined. According to the shoreline angles and elevation values from terraces it was considered to be drawn MIS 5 and MIS 7 levels.

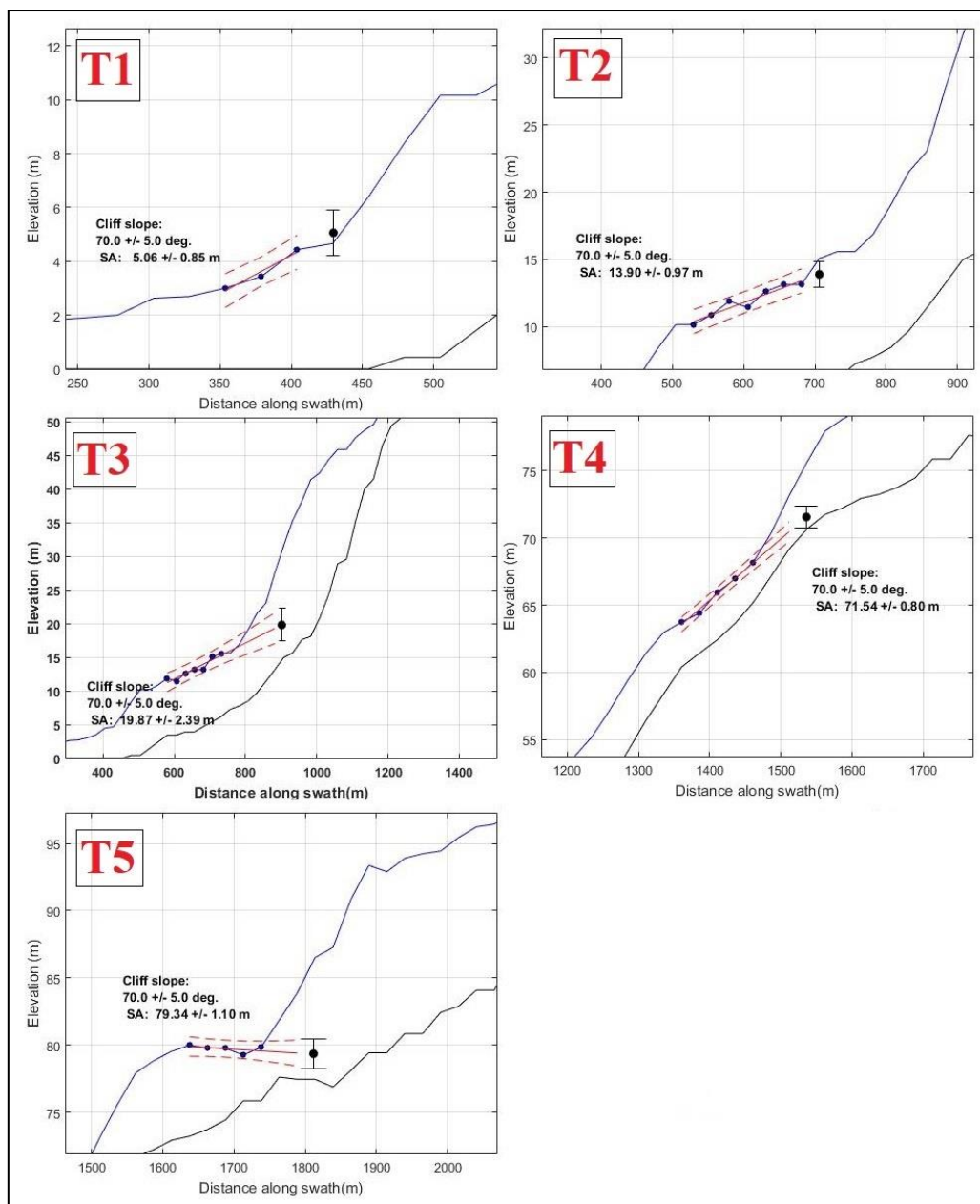


Figure 4.2 : TerraceM results of Cape Carpaz, shoreline angles on profiles.

4.1.2 Dipkarpaz

The Dipkarpaz region is located at the easternmost part of the island. The geology of the region forms Quaternary aged Apalos-Athalassa formation with biocalcarenites, sandstones, sandy marls and conglomerates. Terrace deposits consist of limestones, sand and gravel. I employed three swath profiles that across well preserved cliffs of the paleo-shorelines. Accordingly, I identified each swath profiles 2 levels of paleo-shorelines up to averages of 85 meters (Fig.4.3).

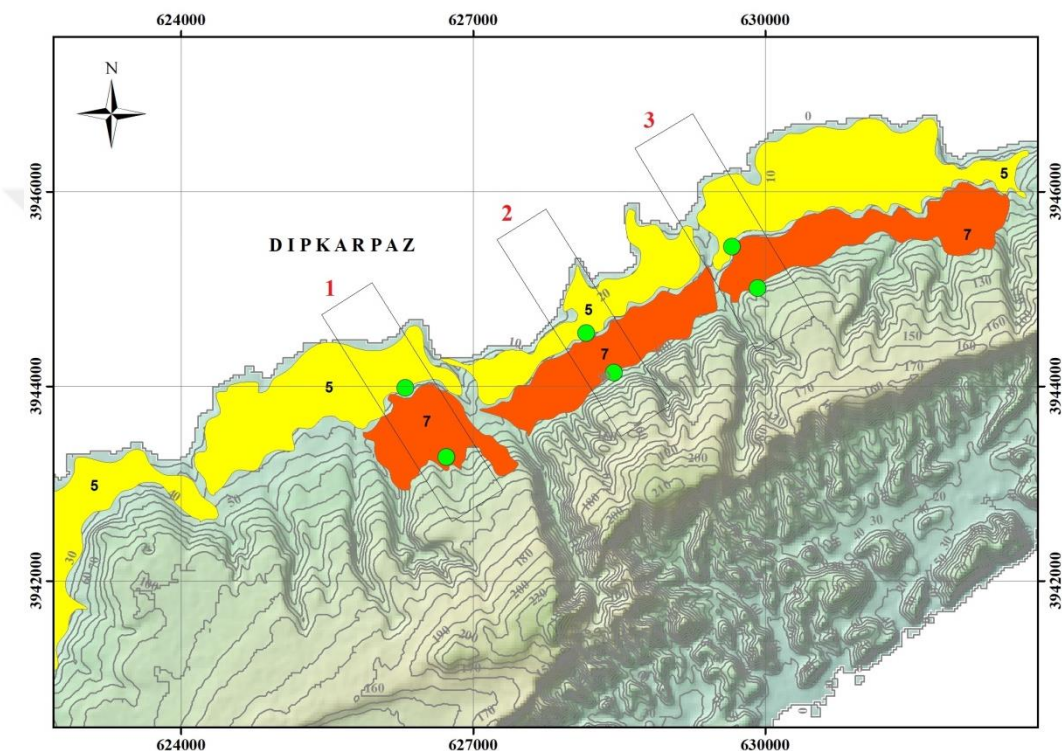


Figure 4.3 : Marine terraces and shoreline angles of Dipkarpaz.

In the first swath profile of Dipkarpaz, elevation values of three terrace surfaces and two shoreline angle values of these terraces are produced in Terracem (Fig.4.4) were seen at (T1) 29.58 ± 1.07 m. and (T2) 85.83 ± 1.26 meters a.s.l.

In the second swath profile elevation values of shoreline angles are (T1) 19.18 ± 2.25 m. and (T2) 81.10 ± 1.96 meters a.s.l. In the third swath profile (T1) 37.56 ± 5.67 m. and (T2) 84.46 ± 1.00 meters above the sea level. Shoreline angles of terraces are shown in green dots. According to the shoreline angles and elevation values from terraces it was considered to be drawn MIS 5 and MIS 7 levels.

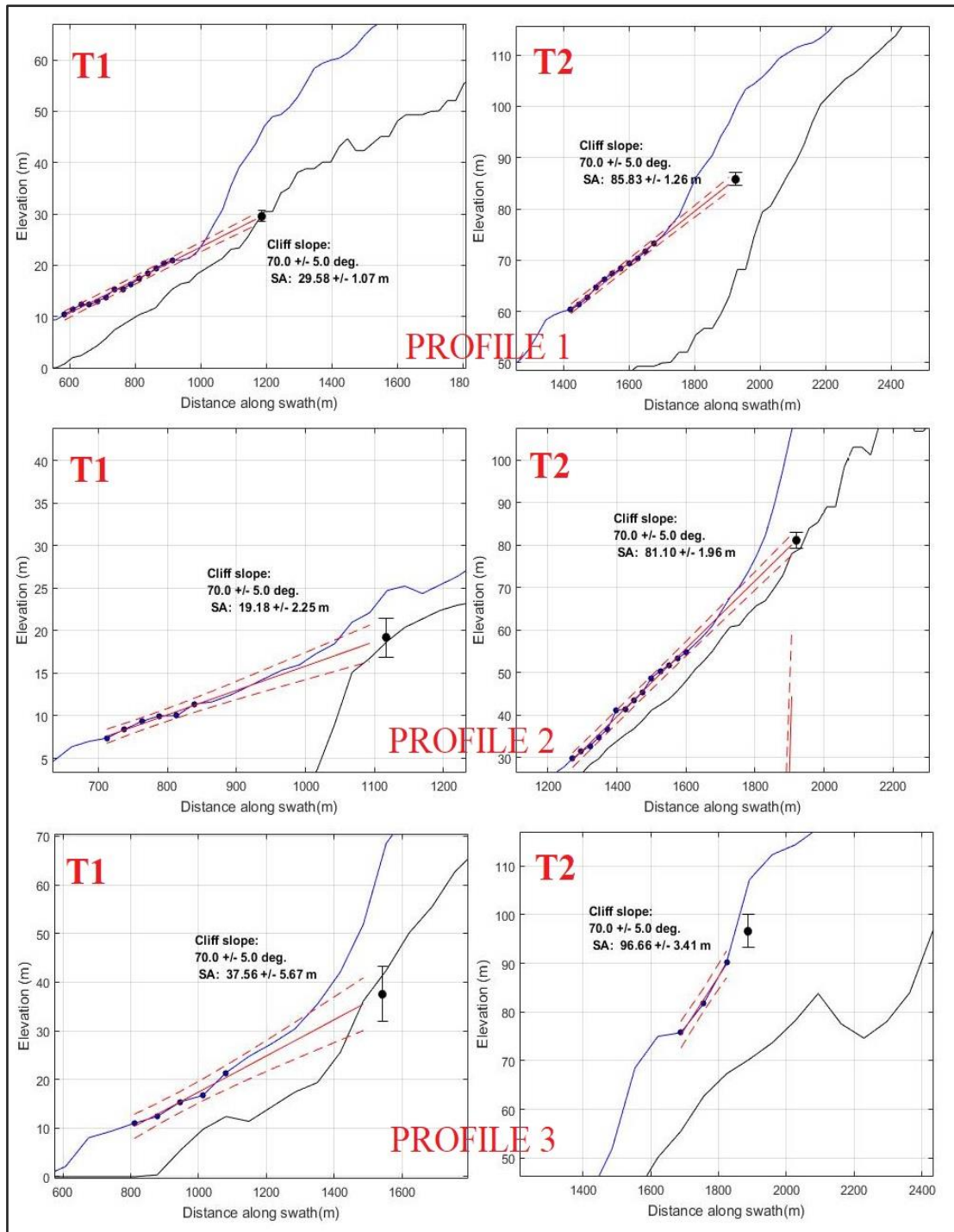


Figure 4.4 : TerraceM results of Cape Carpez, shoreline angles on profiles.

4.1.3 Yeni Erenköy

The Yeni Erenköy region is located at the eastern part of the island. The geology of the region forms Quaternary aged biocalcarenes, sandstones, sandy marls and conglomerates. Terrace deposits consist of limestones, sand and gravel. I employed four swath profiles that across well preserved cliffs of the paleo-shorelines (Fig.4.5).

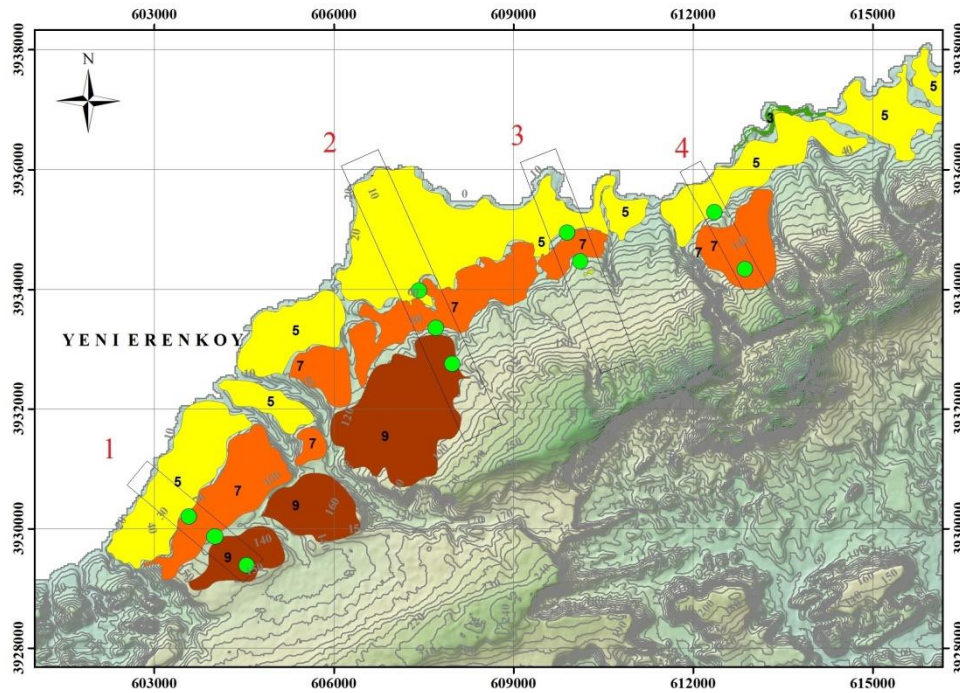


Figure 4.5 : Marine terraces and shoreline angles of Yeni Erenköy.

In the first swath profile of Yeni Erenköy, three shoreline angle values are produced in Terracem (Fig.4.6) were seen at (T1) 9.56 ± 3.69 m, (T2) 27.47 ± 2.97 and (T3) 130.73 ± 13.96 m meters a.s.l.

In the second swath profile elevation values of shoreline angles are (T1) 25.54 ± 10.52 m, (T2) 81.53 ± 2.10 and (T3) 132.38 ± 2.10 meters a.s.l.

In the third swath profile (T1) 10.05 ± 1.70 m. and (T2) 36.40 ± 1.75 meters above the sea level.

In the fourth swath profile elevation values of shoreline angles are (T1) 49.67 ± 5.57 m, (T2) 118.33 ± 0.99 and (T3) 162.90 ± 3.02 meters a.s.l.

Shoreline angles of terraces are shown in green dots. According to the shoreline angles and elevation values from terraces it was considered to be drawn MIS 5, MIS 7 and MIS 9 levels.

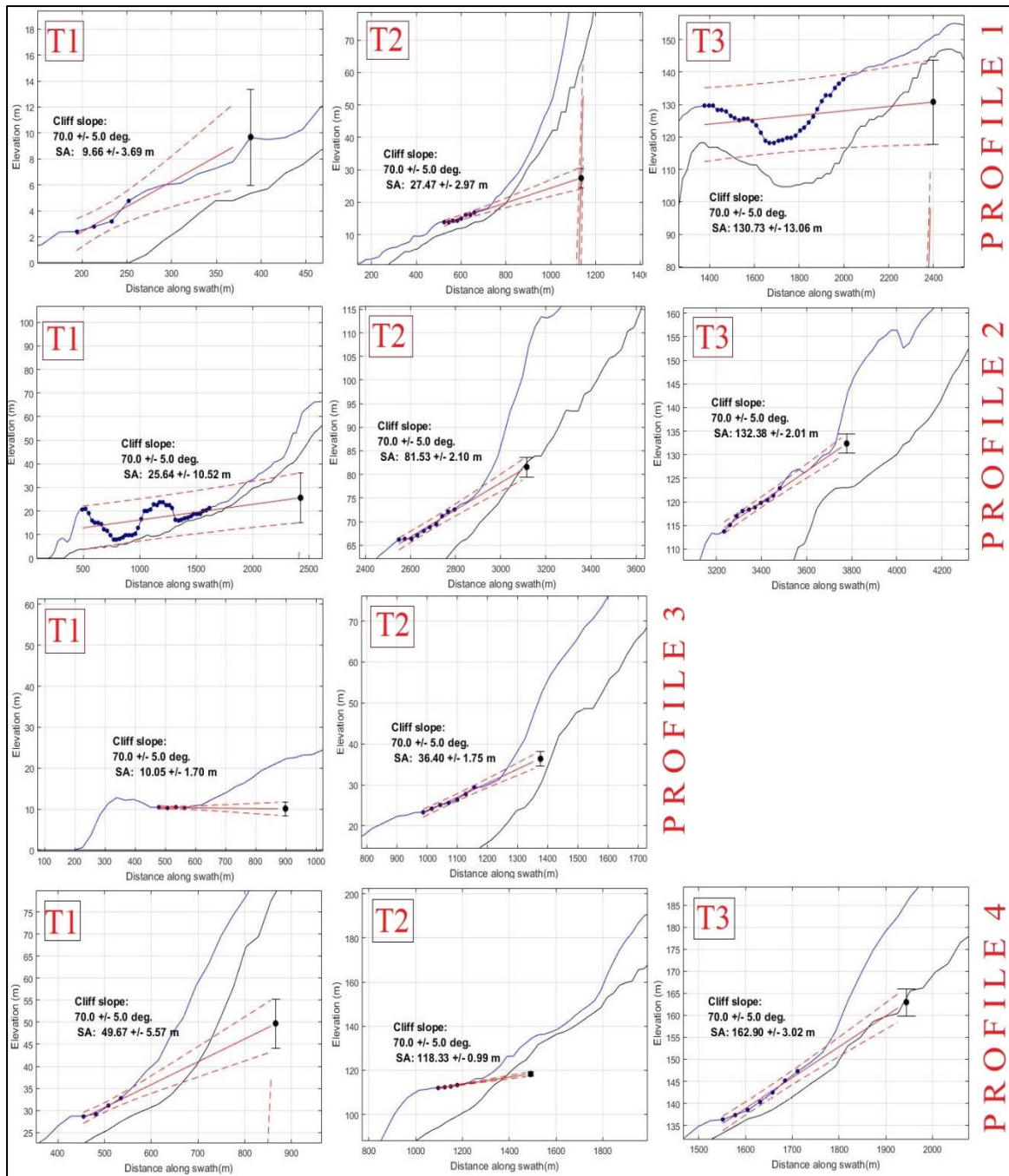


Figure 4.6 : TerraceM results of Yeni Erenköy, shoreline angles on profiles.

4.1.4 Tatlisu

The Tatlisu is located at the north-eastern of the island. The geology of the region forms Middle Miocene aged Kyrethia formation with greywackes, marls, sandstones, Stones and basal conglomerates. Quaternary aged terrace deposits consist of calcarenites, sands and gravels. I employed 8 swath profiles that across well preserved cliffs of the paleo-shorelines (Fig.4.7).

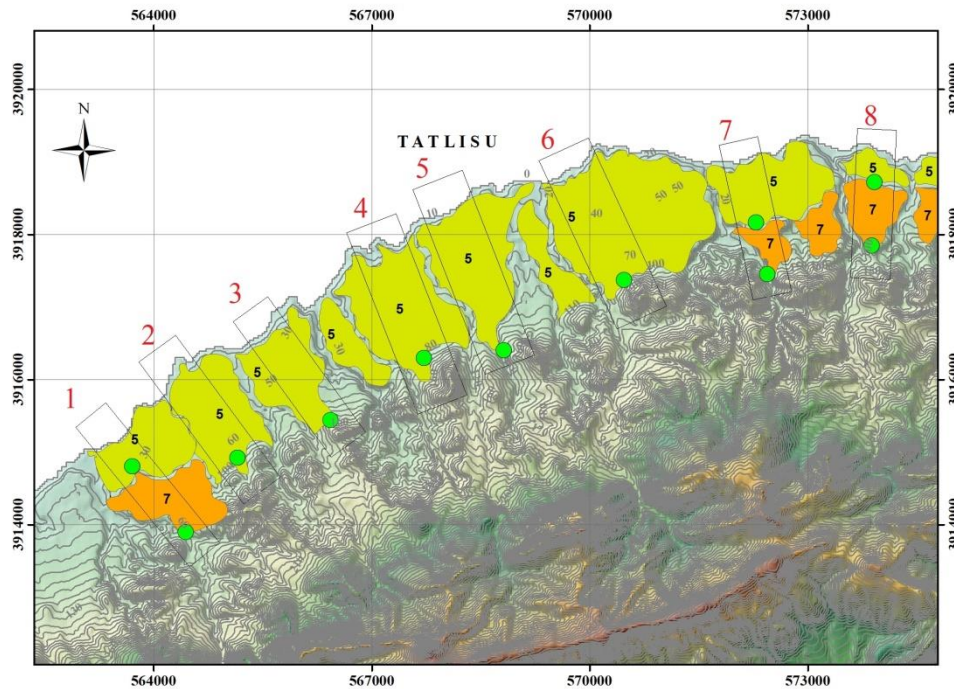


Figure 4.7 : Marine terraces and shoreline angles of Tatlisu.

In the first swath profile of Tatlisu, two shoreline angle values are produced in Terracem (Fig.4.8) were seen at (T1) 27.42 ± 1.00 m and (T2) 83.22 ± 1.10 meters a.s.l.

In the 2nd swath profile elevation value of shoreline angle is (T1) 58.32 ± 3.18 meters above the sea level.

In the 3rd and 4th swath profiles elevation of shoreline angles are (T1) 94.67 ± 4.67 meters above the sea level.

In the 5th swath profile elevation value of shoreline angle is (T1) 88.73 ± 1.83 meters above the sea level.

In the 6th swath profile elevation value of shoreline angle is (T1) 73.72 ± 2.59 meters above the sea level.

In the 7th swath profile elevation values of shoreline angles are (T1) 70.34 ± 2.66 m. and (T2) 115.86 ± 1.01 meters above the sea level.

Lastly in the 8th swath profile elevation values of shoreline angles are (T1) 40.14 ± 4.03 m. and (T2) 90.60 ± 0.63 meters above the sea level. Shoreline angles of terraces are shown in green dots. According to the shoreline angles and elevation values from terraces it was considered to be drawn MIS 5 and MIS 7 levels.

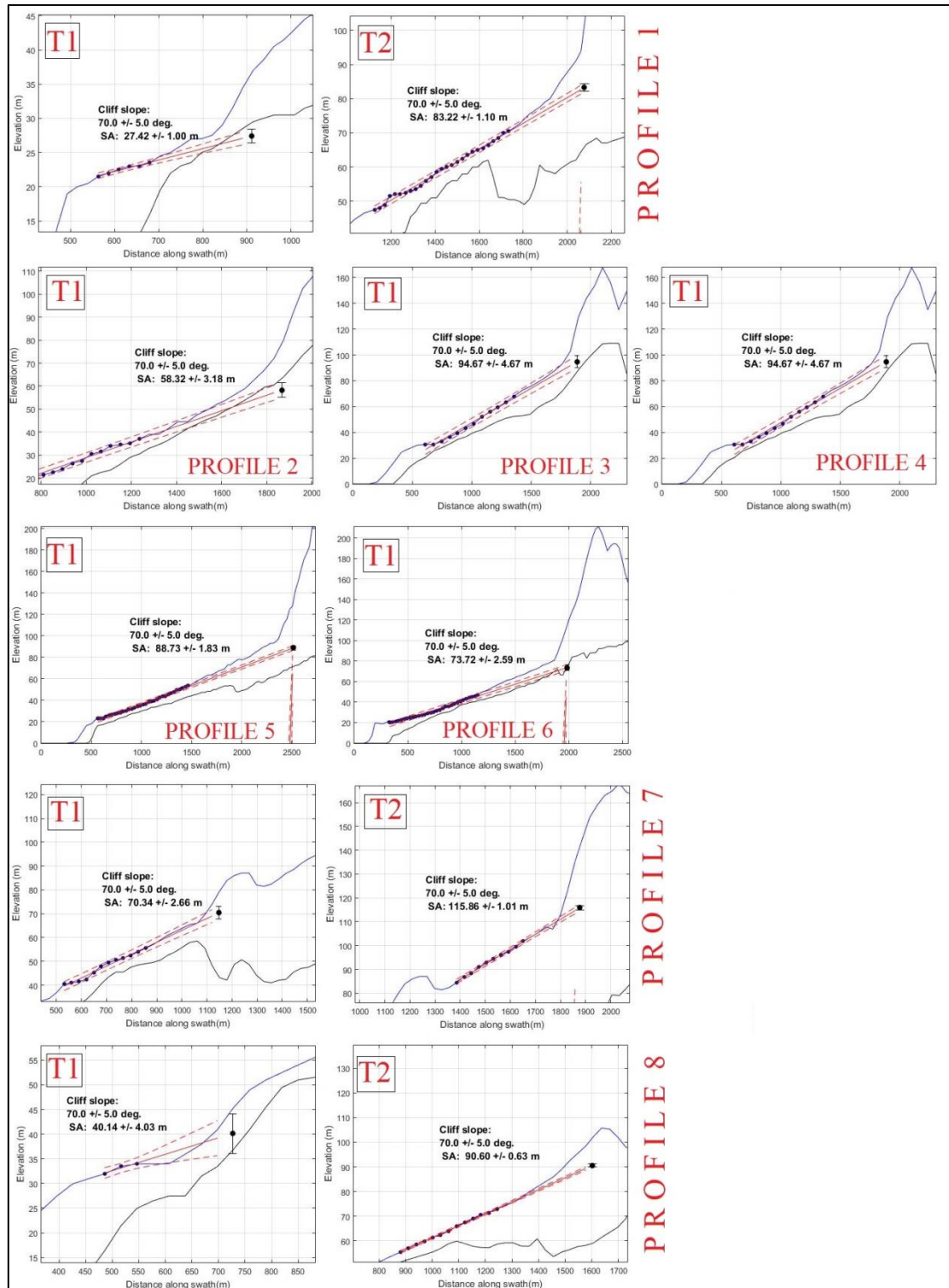


Figure 4.8 : TerraceM results of Tatlisu, shoreline angles on profiles.

4.1.5 Kyrenia

The Kyrenia is located at the northern part of the island. The geology of the region forms mainly Quaternary aged terrace deposits consist of calcarenites, sands and gravels. I employed 4 swath profiles that across well preserved cliffs of the paleo-shorelines (Fig.4.9). The MIS 5 level terrace deposits extend about 2.5 km from the shoreline.

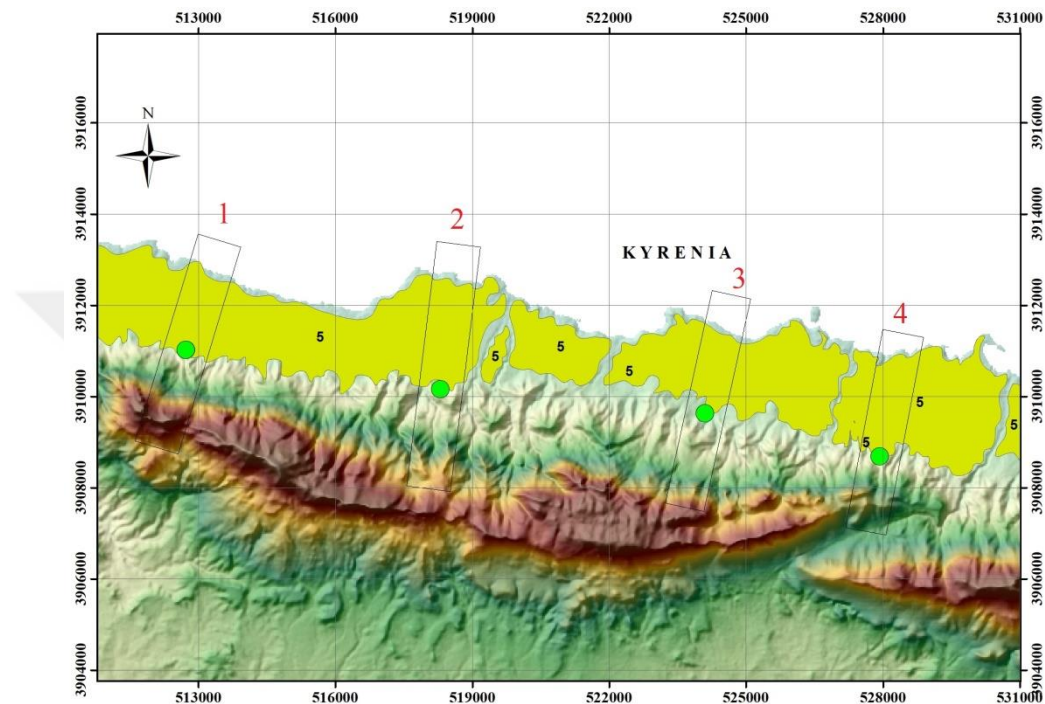


Figure 4.9 : Marine terraces and shoreline angles of Kyrenia.

In the first swath profile of Kyrenia, one shoreline angle value is produced in Terracem (Fig.4.10) were seen at (T1) 50.70 ± 2.20 meters a.s.l.

In the 2nd swath profile elevation value of shoreline angle is (T1) 62.98 ± 0.96 meters above the sea level.

In the 3rd swath profile elevation of shoreline angle is (T1) 52.31 ± 3.89 meters above the sea level.

In the 4th swath profile elevation value of shoreline angle is (T1) 63.48 ± 6.14 meters above the sea level.

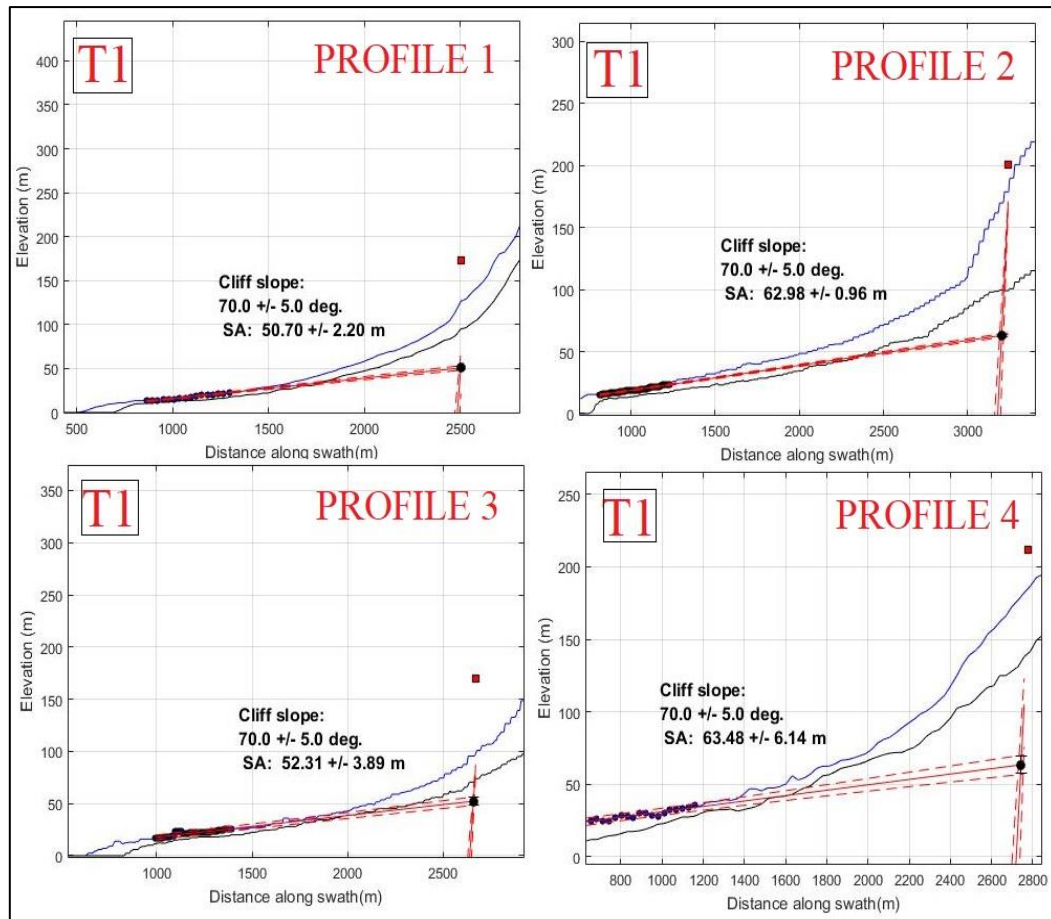


Figure 4.10 : TerraceM results of Kyrenia, shoreline angles on profiles.

4.1.6 Akdeniz

The Akdeniz region is located at the northwestern part of the island. The geology of the region forms Quaternary aged Apalos-Athalassa formation with biocalcarenites, sandstones, sandy marls and conglomerates. In addition there are Holocene aged Alluvium- Colluvium formation with sands, silts, clays and gravels. Terraces between the two faults and levels ranging from MIS 5 to MIS 13 were identified in this area (Fig.4.11).

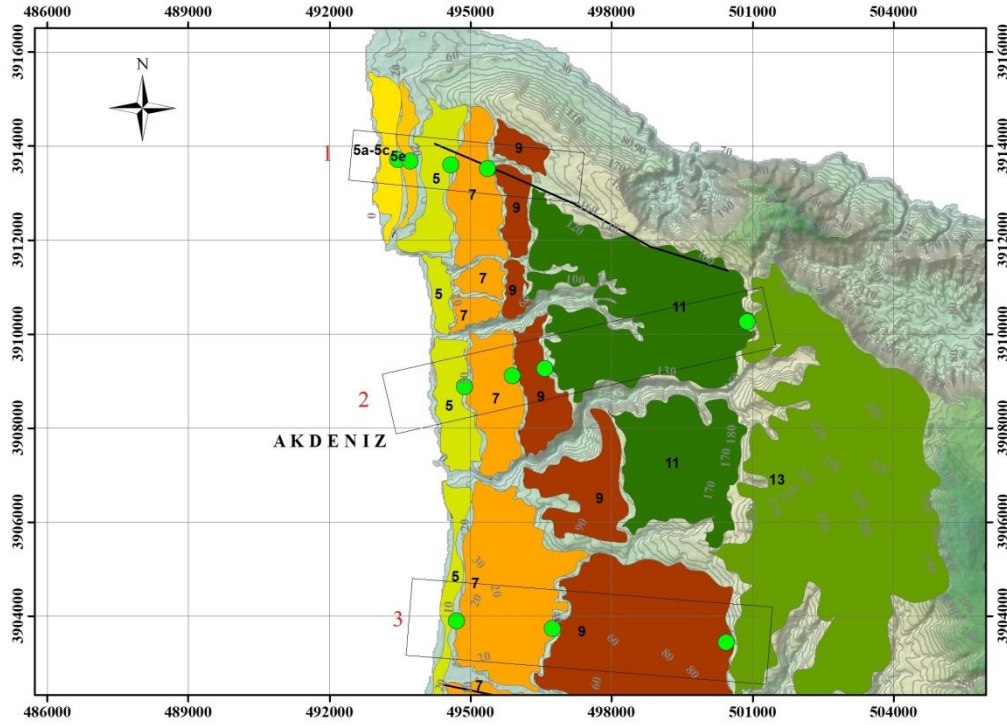


Figure 4.11 : Marine terraces and shoreline angles of Akdeniz.

In the first swath profile of Akdeniz, four shoreline angle values are produced in Terracem (Fig.4.12) were seen at (T1) $13.90 \pm 0.99\text{m}$. , (T2) $21.58 \pm 0.49 \text{ m}$. , (T3) $42.30 \pm 0.83 \text{ m}$. and (T4) $81.62 \pm 1.19 \text{ meters a.s.l}$.

In the second swath profile elevation values of shoreline angles are (T1) $28.41 \pm 5.07 \text{ m}$. , (T2) 45.07 ± 5.11 and (T3) 89.49 ± 0.74 and (T4) $146.14 \pm 3.25 \text{ meters a.s.l}$.

In the third swath profile (T1) $10.05 \pm 1.70 \text{ m}$. and (T2) $36.40 \pm 1.75 \text{ meters above the sea level}$.

In the fourth swath profile elevation values of shoreline angles are (T1) $4.32 \pm 0.74 \text{ m}$. , (T2) 23.41 ± 4.16 and (T3) $84.10 \pm 4.95 \text{ meters a.s.l}$.

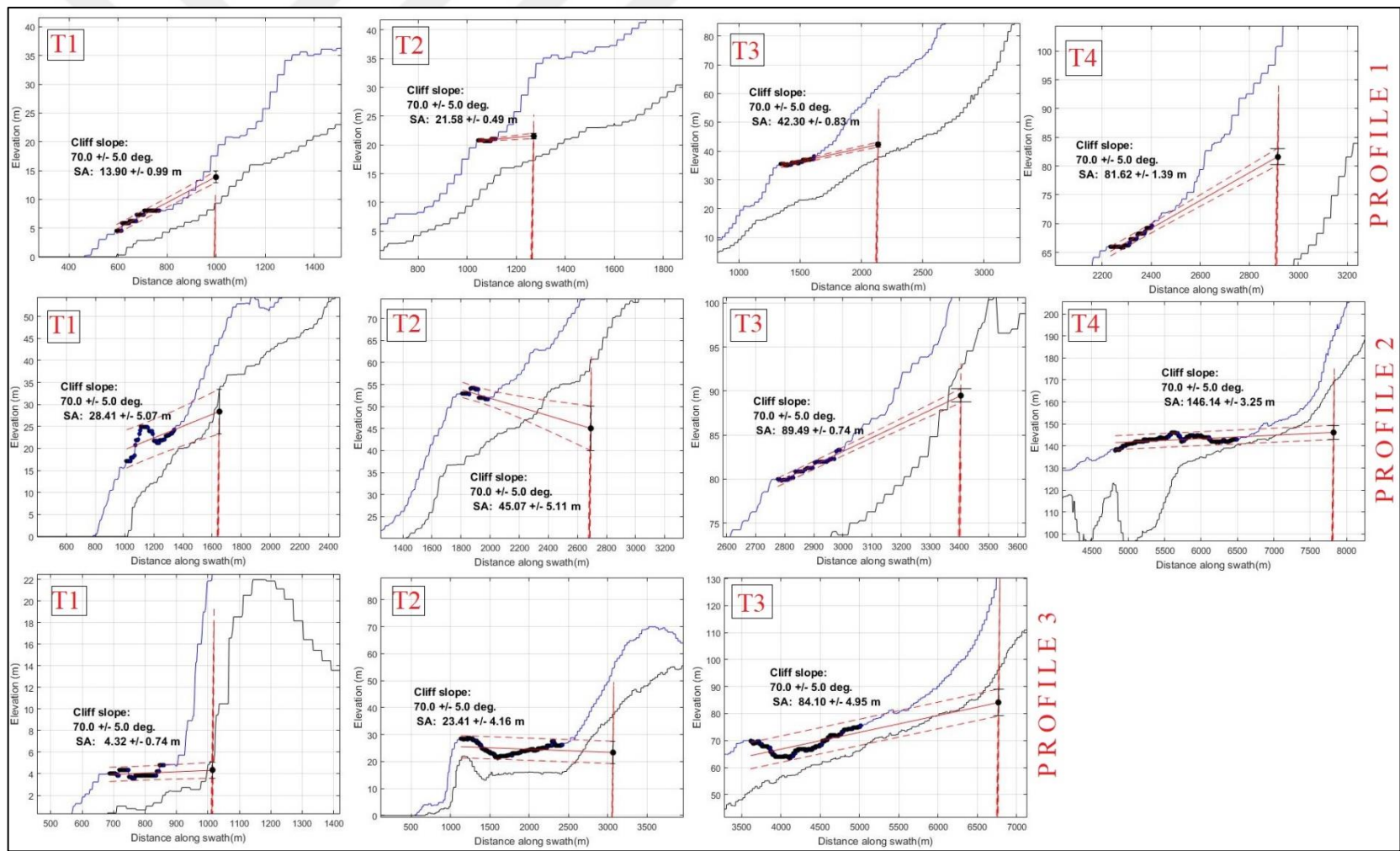


Figure 4.12 : TerraceM results of Akdeniz, shoreline angles on profiles.

4.2 Marine Terraces in Southern Cyprus

4.2.1 Yeronisos

Yeronisos is located at the southwest part of the island. The geology of the region forms Quaternary aged terrace deposits with calcarenites, sands and gravels. I employed 3 swath profiles that across cliffs of the paleo-shorelines (Fig.4.13).

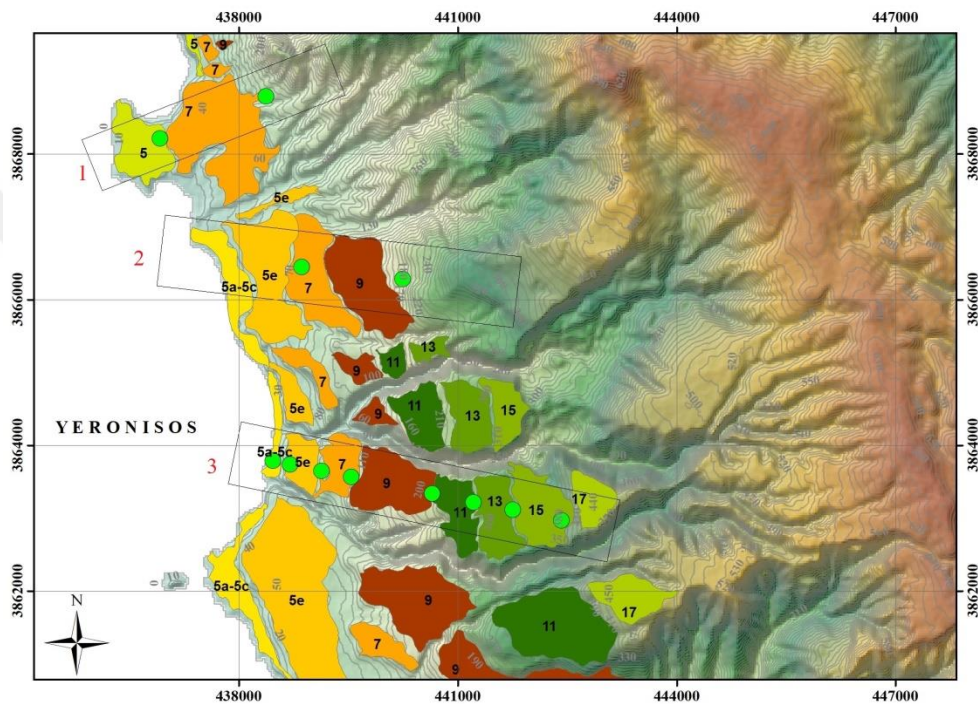


Figure 4.13 : Marine terraces and shoreline angles of Yeronisos.

In the first swath profile of Yeronissos, two shoreline angle values are produced in Terracem (Fig.4.14) were seen at (T1) 19.85 ± 1.47 m. , (T2) 42.58 ± 0.75 meters a.s.l.

In the second swath profile elevation values of shoreline angles are (T1) 68.91 ± 3.22 m. , (T2) 168.58 ± 1.34 m. a.s.l.

In the third swath profile (T1) 12.76 ± 1.36 m. , (T2) 45.46 ± 2.97 m. , (T3) 69.67 ± 1.08 m. , (T4) 98.45 ± 1.44 m. , (T5) 207.31 ± 1.77 m. , (T6) 258.66 ± 2.38 m. , (T7) 296.05 ± 0.99 m. and (T8) 357.96 ± 3.05 meters above the sea level (Fig.4.15).

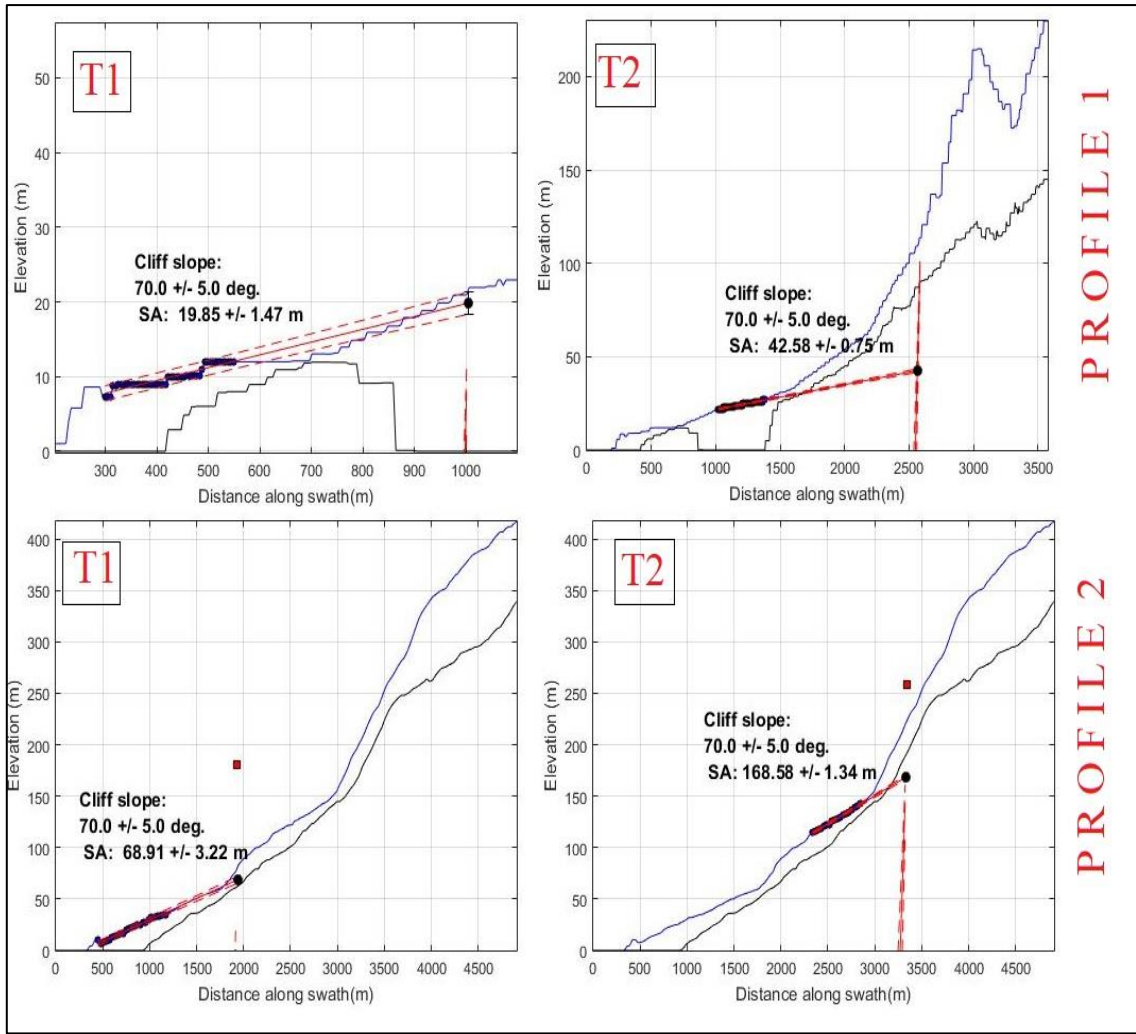


Figure 4.14 : TerraceM results of Yeronisos, shoreline angles on profiles.

PROFILE 3

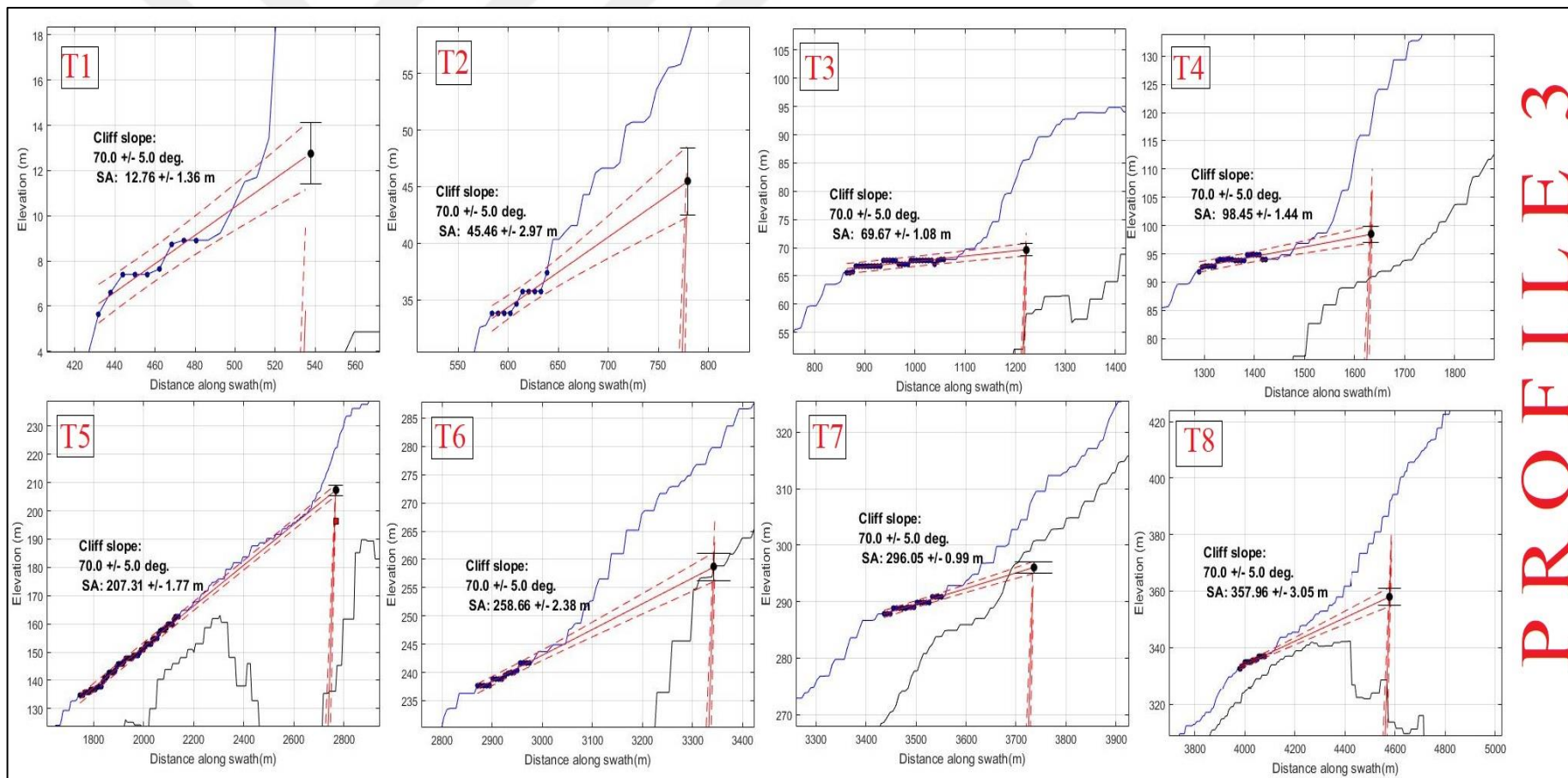


Figure 4.15 : TerraceM results of Yeronisos, Profile 3.

4.2.2 Paphos

Paphos is located at the southwest part of the island. The geology of the region forms Quaternary aged terrace deposits with calcarenites, sands and gravels. I employed 3 swath profiles that across cliffs of the paleo-shorelines.

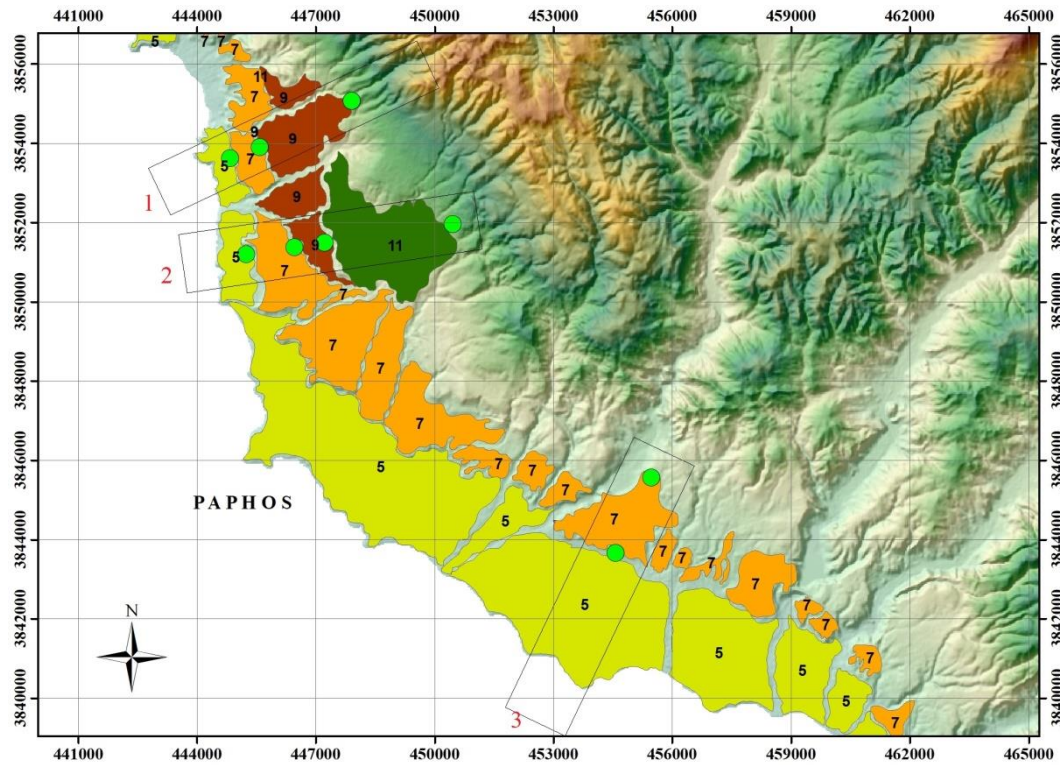


Figure 4.16 : Marine terraces and shoreline angles of Paphos.

In the first swath profile of Yeronissos, two shoreline angle values are produced in Terracem (Fig.15) were seen at (T1) 19.85 ± 1.47 m. , (T2) 42.58 ± 0.75 meters a.s.l.

In the second swath profile elevation values of shoreline angles are (T1) 68.91 ± 3.22 m. , (T2) 168.58 ± 1.34 m. a.s.l.

In the third swath profile (T1) 12.76 ± 1.36 m. , (T2) 45.46 ± 2.97 m. , (T3) 69.67 ± 1.08 m. , (T4) 98.45 ± 1.44 m. , (T5) 207.31 ± 1.77 m. , (T6) 258.66 ± 2.38 m. , (T7) 296.05 ± 0.99 m. and (T8) 357.96 ± 3.05 meters above the sea level.

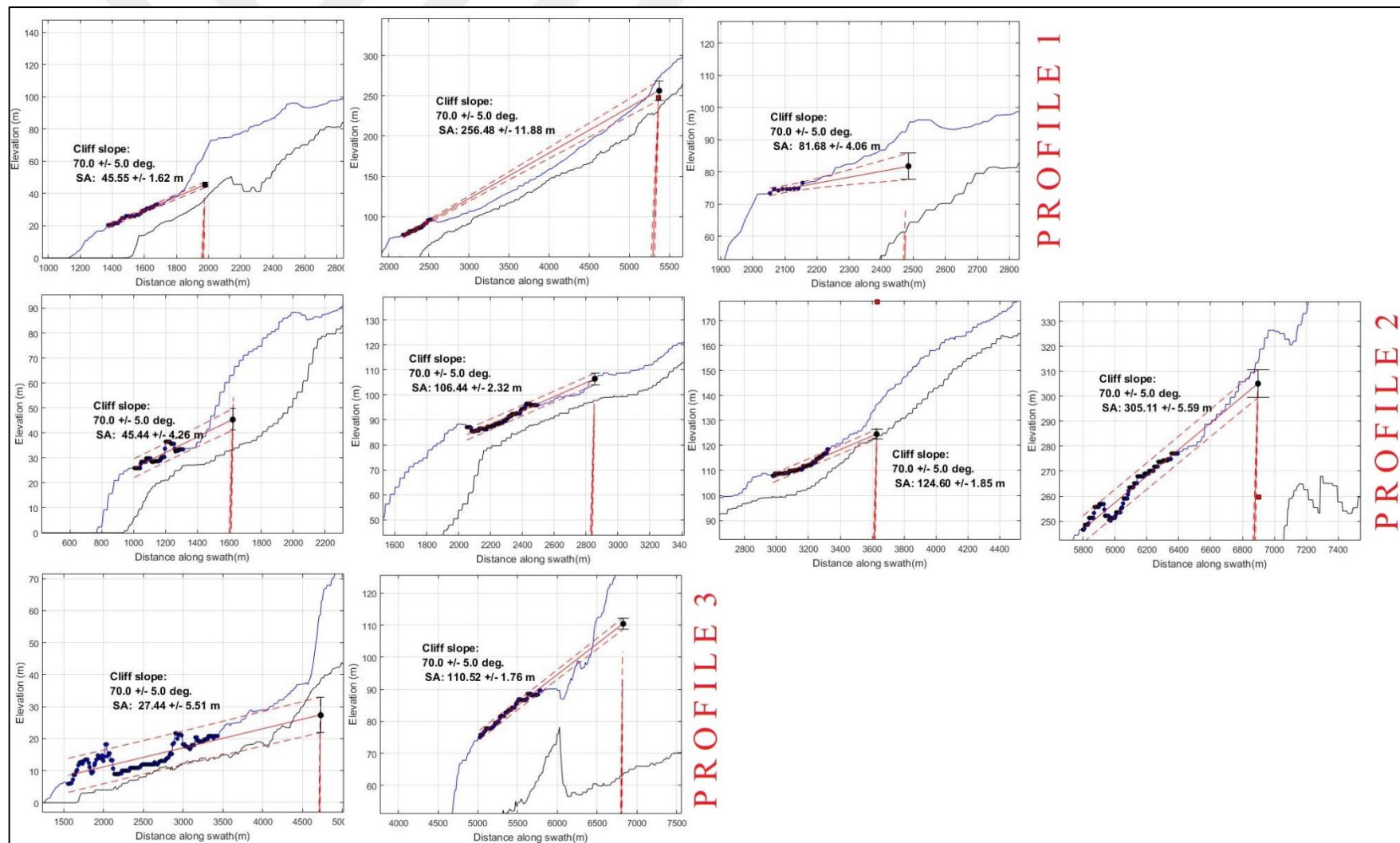


Figure 4.17 : TerraceM results of Paphos.



5. DISCUSSION

5.1 Implications For Rate And Deformation Pattern In The Northern Cyprus

In five regions studied in northern Cyprus, mainly MIS 5, MIS 7, MIS 9 and MIS 11 marine terrace levels defined in TerraceM. In the terraces overlooking the north of the island, the MIS 5 surfaces cover large areas, while in the southern areas it observed that they are located only on the coastline (Fig.5.1).

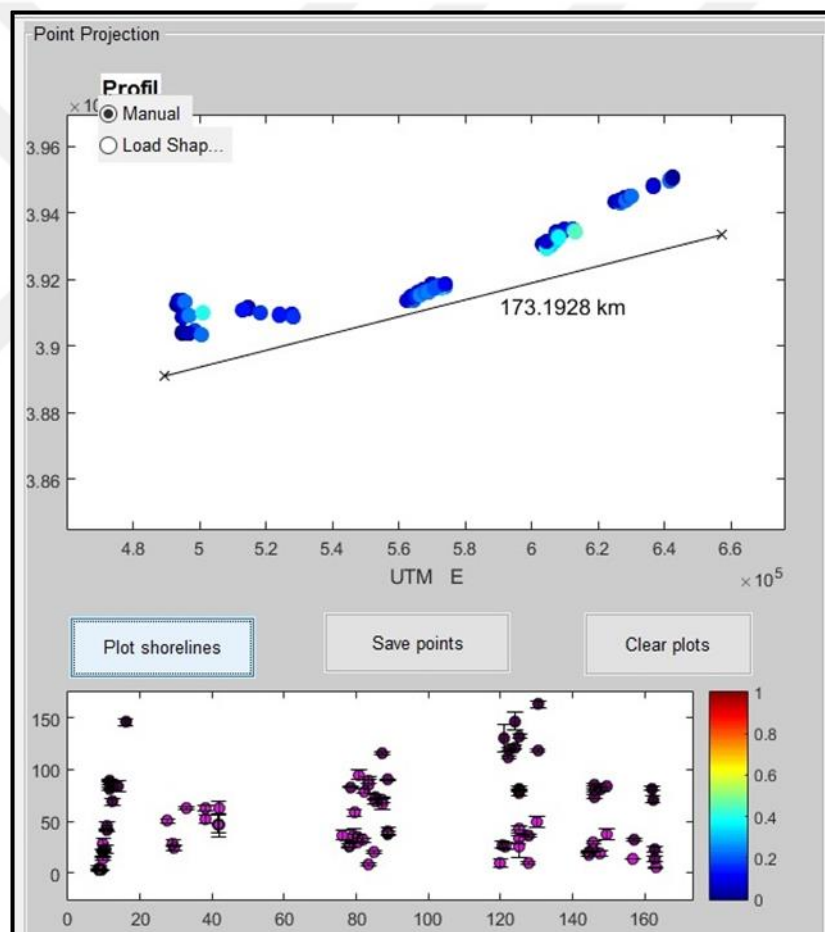


Figure 5.1: Projection of the shoreline angle elevations, Northern Cyprus.

The coseismic uplift in the Cape Karpaz can be supported by the five different terraces (Fig.4.1) were seen at sea level (T1) 5.55 ± 0.90 m, (T2) 13.72 ± 2.69 m, (T3) 22.53 ± 2.58 m, (T4) 71.33 ± 3.19 m and (T5) 82.02 ± 2.25 meters above the sea

level on the swath profile. Accordingly, temporal uplift rates calculated 0.23 ± 0.00 mm/yr (a) and 0.22 ± 0.00 (b) in Cape Karpaz.

In Dipkarpaz, MIS 5 and MIS 7 levels were observed at an average elevation of 30 m and 80 meters. The uplift rate calculated according to the highest paleo cliff (Fig.4.4) where MIS7 level is found is 0.44 ± 0.02 mm/yr (a) and 0.41 ± 0.02 mm/yr (b).

The paleo-cliff elevations of the Yeni Erenköy region, calculated from the swath profile where 3 terrace levels (Fig.4.6) can be seen, are (T1) 9.56 ± 3.69 m, (T2) 27.47 ± 2.97 and (T3) 130.73 ± 13.96 m meters a.s.l.meters. Accordingly, the uplift rates calculated 0.48 ± 0.01 mm/yr (a) and 0.47 ± 0.01 (b) mm/yr.

The second terrace level (MIS 7) could be calculated in the 1st, 7th and 8th profiles, although eight swath profiles (Fig.4.7) taken in the Tatlısu region show predominantly single terrace level (MIS 5). The levels shown in profile 7 (Fig.4.8) are (T1) 70.34 ± 2.66 m. and (T2) 115.86 ± 1.01 meters the calculated uplift rates are 0.52 ± 0.02 mm/yr (a) and 0.49 ± 0.01 mm/yr (b).

The steepness of the terrace profiles in the Kyrenia range is quite striking, with the shoreline angle positions of the terraces almost corresponding to the coastline on the Pliocene. Single terrace level was seen in all swath profiles taken in Kyrenia Region. These single level terraces are mapped to MIS 5 (Fig.4.9). The paleo-cliff elevations of these levels were calculated as 50.70 ± 2.20 m, 62.98 ± 0.96 m, 49.47 ± 2.89 m and 63.48 ± 6.14 meters (Fig.4.10). The uplift rates calculated according to the Profile 4 are 0.47 ± 0.02 mm/yr (a) and 0.46 ± 0.03 mm/yr (b), respectively.

5.2 Implications For Rate And Deformation Pattern In The Southern Cyprus

For two regions in southern Cyprus, maps of marine terraces were created with reference to the MIS levels given by Zomeni (2012). The uplift rate values in Yeronisos and Paphos are in line with the values (0.63 mm/a) given by the Zomeni for the same region.

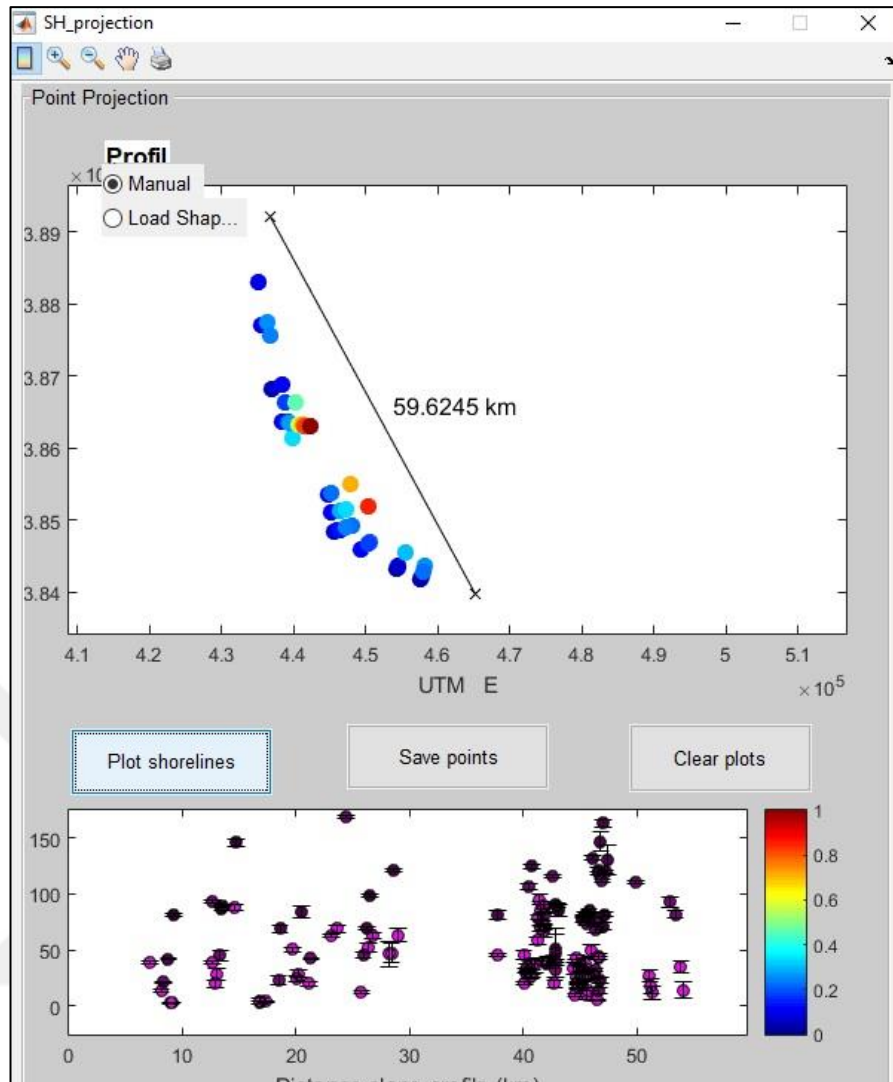


Figure 5.2: Projection of the shoreline angle elevations, Paphos and Yeronisos.

The highest terrace level in Yeronisos was seen as MIS 15 at 357.96 ± 3.05 m elevation. MIS 5a is 12.76 ± 1.36 m, MIS 5c is 45.46 ± 2.97 m, MIS 5e is 69.67 ± 1.08 m, MIS 7 is 98.45 ± 1.44 m, MIS 9 is 207.31 ± 1.77 m, MIS 11 is 258.66 ± 0.99 m, MIS 13 is 296.05 ± 0.99 m. The uplift rate calculated according to MIS 15 is 0.64 ± 0.03 mm/yr (a).

The seismic intensity in the Paphos region supports the uplifted terraces. In Paphos, it is seen that the MIS 5 terraces entered about 30 m from the shore. MIS 5 and MIS 7 levels are generally seen here, but MIS 9 in Kissonergra (Fig.4.16, Profile 1) and MIS 11 in Chlorakas (Fig.4.16) are observed. The paleo-cliff elevations of Profile 2 are (T1) 68.91 ± 3.22 m, (T2) 168.58 ± 1.34 m. The uplift rate calculated according to MIS 11 is 0.74 ± 0.01 mm/yr (a).

5.3 Distribution Of Quaternary Deformation On The Cyprus Island

I calculated uplift rate according to highest marine terraces (Table 5.1) to get long term uplift rate and I also calculate uplift rate variation through time according to time and elevation difference between different terrace levels (Table 5.2). Nevertheless in order to find the pattern (Figure 5.3) I use MIS 5e level as a reference level all along the northern and southern coasts of the Cyprus.

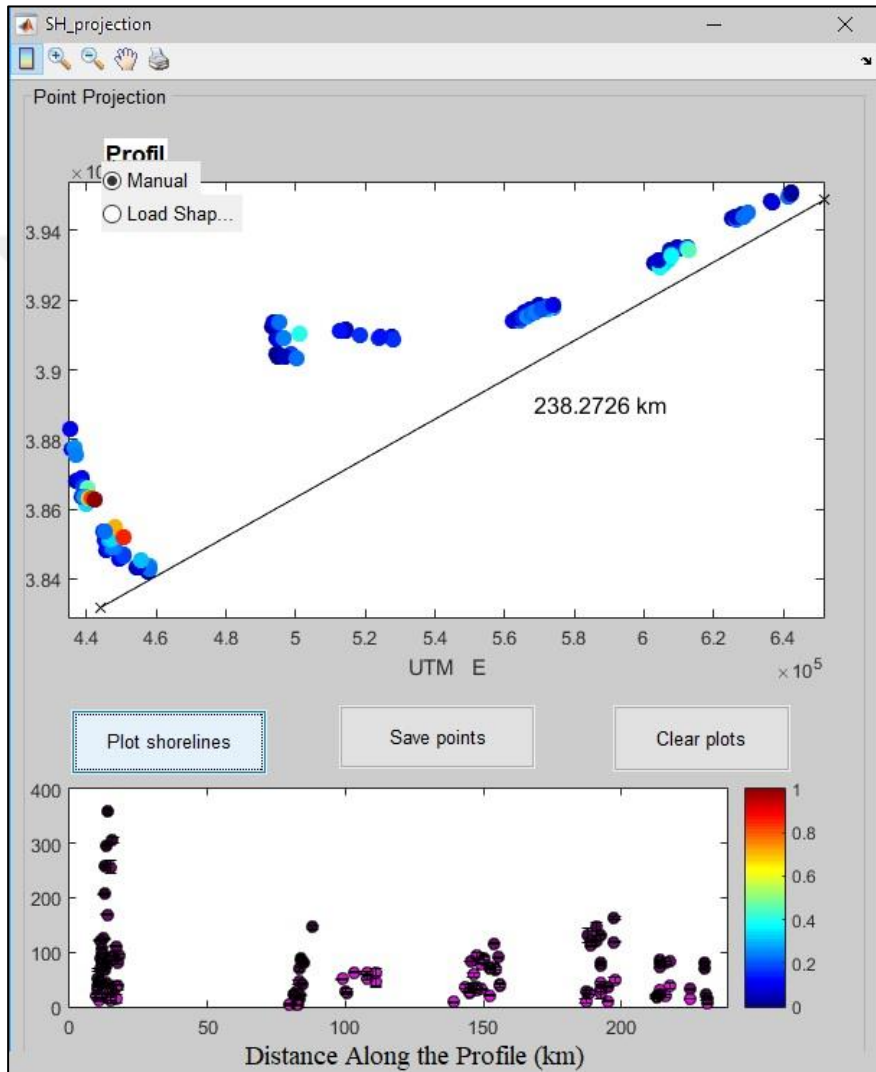


Figure 5.3: Projection of the shoreline angle elevations, Cyprus.

Table 5.1 : Temporal Marine Isotope Stages, total displacements and uplift rates to highest elevation of terraces.

Morphotectonic Segment	Highest MIS Stage	MIS Age (ka)	Shoreline Angle (m)	Sea-Level Highstand Elevation (a) (m)	Sea-Level Highstand Elevation (b) (m)	Total Displacement (a) (m)	Total Displacement (b) (m)	Uplift Rate (mm/a) (a)	Uplift Rate (mm/a) (b)
Cape Karpaz	9	334 ± 4	79,34 ± 1,10	+4	+5	75,34 ± 1,1	74,34 ± 1,10	0,23 ± 0,00	0,22 ± 0,00
Dip Karpaz	7	244	96,66 ± 3,41	-11 ± 4	-3,5	107,66 ± 5,26	100,16 ± 3,41	0,44 ± 0,02	0,41 ± 0,02
Yeni Erenköy	9	334 ± 4	162,90 ± 3,02	+4	+5	158,90 ± 3,02	157,90 ± 3,02	0,48 ± 0,01	0,47 ± 0,01
Tatlısu	7	244	115,86 ± 1,01	-11 ± 4	-3,5	126,86 ± 4,13	119,36 ± 1,01	0,52 ± 0,02	0,49 ± 0,01
Kyrenia	5	124	62,98 ± 0,96	+5 ± 2	+6 ± 3	57,98 ± 2,22	56,98 ± 3,15	0,47 ± 0,02	0,46 ± 0,03
Akdeniz	11	410	146,14 ± 3,25	+2 ± 1	+6	144,14 ± 3,40	140,14 ± 3,25	0,35 ± 0,01	0,34 ± 0,01
Yeronisos	15	570	168,58 ± 1,34	-8 ± 2	?	176,58 ± 2,41	-	0,31 ± 0,00	-
Paphos	11	410	305,11 ± 5,59	+2 ± 1	?	303,11 ± 5,68	-	0,74 ± 0,01	-

(a) According to Siddal et al. 2006
(b) According to Zomeni, 2012

Table 5.2 : Temporal Marine Isotope Stages, total displacements and uplift rates to MIS 5 level terraces.

Morphotectonic Segment	Highest MIS Stage	MIS Age (ka)	Shoreline Angle (m)	Sea-Level Highstand Elevation (a) (m)	Sea-Level Highstand Elevation (b) (m)	Total Displacement (a) (m)	Total Displacement (b) (m)	Uplift Rate (mm/a) (a)	Uplift Rate (mm/a) (b)
Cape Karpaz	5	124	32,09 ± 1,15	+5 ± 2	+6 ± 3	27,09 ± 2,31	26,09 ± 3,21	0,22 ± 0,02	0,21 ± 0,03
Dip Karpaz	5	124	29,58 ± 1,07	+5 ± 2	+6 ± 3	24,58 ± 2,27	23,58 ± 3,19	0,20 ± 0,02	0,19 ± 0,03
Yeni Erenköy	5	124	25,64 ± 1,52	+5 ± 2	+6 ± 3	20,64 ± 2,51	19,64 ± 3,36	0,17 ± 0,02	0,16 ± 0,03
Tatlısu	5	124	73,72 ± 2,59	+5 ± 2	+6 ± 3	68,72 ± 3,27	67,72 ± 3,96	0,55 ± 0,03	0,55 ± 0,04
Kyrenia	5	124	63,48 ± 6,14	+5 ± 2	+6 ± 3	58,48 ± 6,46	57,48 ± 6,83	0,47 ± 0,05	0,46 ± 0,07
Akdeniz	5	124	13,90 ± 0,99	+5 ± 2	+6 ± 3	8,90 ± 2,23	7,90 ± 3,16	0,07 ± 0,02	0,06 ± 0,03
Yeronisos	5	124	68,91 ± 3,22	+5 ± 2	+6 ± 3	63,91 ± 3,79	62,91 ± 4,40	0,52 ± 0,03	0,51 ± 0,04
Paphos	5	124	45,55 ± 1,62	+5 ± 2	+6 ± 3	40,55 ± 2,57	39,55 ± 3,41	0,33 ± 0,02	0,32 ± 0,03

(a) According to Siddal et al. 2006
(b) According to Zomeni, 2012



6. CONCLUSION

Marine terraces mapped in different regions north and south of the island of Cyprus. The uplift rates for terraces are calculated (Table 3 and Table 4) according to the MIS ages and paleo sea level elevations given by Siddal et al. 2006 and Zomeni 2012. I correlated MIS5, MIS7, MIS9, MIS 11 and MIS 15 highstands based on major marine terrace levels. The north of the island shown predominantly MIS 5 and MIS 7 marine terrace levels. The uplift rates for modern terraces in the north are closer to each other, except for uplift rates in Kyrenia and Akdeniz regions. It can be said that subduction related processes are effective in these regions when long term and short term uplift rates are compared (Table 5.1 and Table 5.2). Topographic analysis of the Akdeniz region shows the presence of uplifted marine terraces between two faults. A shoreline angle elevations of more than 300 meters in the Paphos and Yeronisos regions in the south may be related to the seismic intensity in this region. Practical Application of This Study.



REFERENCES

- Aksu, A.E., Hall, J. & Yaltrak, C.** (2005). Miocene to Recent tectonic evolution of the eastern Mediterranean: New pieces of the old Mediterranean puzzle. *Marine Geology* 221, 1 – 13
- Aksu, A.E., Hall, J. & Yaltrak, C.** (2008). Miocene–Recent evolution of Anaximander Mountain and Finike Basin at the junction of Hellenic and Cyprus Arcs, Eastern Mediterranean. *Marine Geology*, doi: 10.1016/j.margeo.2008.04.008
- Aksu, A.E., Calon, T.J., Hall, J., Mansfield, S., Yaşar, D.,** (2005). The Cilicia–Adana basin complex, Eastern Mediterranean: Neogene evolution of an active fore-arc basin in an obliquely convergent margin. *Marine Geology* 221, 121–159
- Alçıçek, M.C., Ten Veen, J.H. & Özkul, M.** (2006). Neotectonic development of the Çameli Basin, southwestern Anatolia, Turkey. In: Robertson, A.H.F. & Mountrakis, D. (eds), *Tectonic Development of the Eastern Mediterranean Region*. Geological Society, London, Special Publications 260, 591– 611.
- Barka, A., Reilinger, R.,** (1997). Active Tectonics of The Eastern Mediterranean Region: Deduced from GPS, Neotectonic and Seismicity Data. *Annali Di Geofisica*, Vol. XL, N.3, June.
- Ben-Avraham, Z., Garfunkel, Z. & Lazar, M.** (2008). Geology and evolution of the southern Dead Sea Fault with emphasis on subsurface structure. *Annual Review of Earth and Planetary Sciences* 36, 357–387
- Benjamin et al.** (2017). Late Quaternary sea-level changes and early human societies in the central and eastern Mediterranean Basin: An interdisciplinary review.
- Bishop, P.,** (2007). Long-term landscape evolution: linking tectonics and surface processes. *Earth Surf. Process. Landf.* 32 (3), 329e365.
- Bloom, A.L., Broecker, W.S., Chappell, J.M.A., Matthews, R.K., Mesolella, K.J.,** (1974). Quaternary sea level fluctuations on a tectonic coast:

new $^{230}\text{Th}/^{234}\text{U}$ dates from the Huon Peninsula, New Guinea. *Quat. Res.* 4 (2), 185e205.

Bozkurt, E. (2001). Neotectonics of Turkey – a synthesis. *Geodicamica Acta* 14, 3–30.

Caputo, R., Bianca, M., D’Onofrio, R., (2010). Ionian marine terraces of southern Italy: Insights into the Quaternary tectonic evolution of the area. *Tectonics*.

Dewey, J.F., Hempton, M.R., Kidd, W.S.F., Şaroğlu, F., Şengör, A.M.C., (1986). Shortening of continental lithosphere: the neotectonics of eastern Anatolia—a young collision zone. In: Coward, M.P., Ries, A.C. (Eds.), *Collision Tectonics*, Geological Society Special Publication, vol. 19, pp. 3 – 36.

Galili et al. (2015). Late Quaternary beach deposits and archaeological relicts on the coasts of Cyprus, and the possible implications of sea-level changes and tectonics on the early populations.

Gardosh, M.A. & Druckman, Y. (2006). Seismic stratigraphy, structure and tectonic evolution of the Levantine Basin, offshore Israel. In: Robertson, A.H.F. & Mountrakis, D. (eds), *Tectonic Development of the Eastern Mediterranean Region*. Geological Society, London, Special Publications 260, 201– 227.

Garfunkel, Z., Zak, Y. & Freund, R. (1981). Active faulting in the Dead Sea rift. *Tectonophysics* 80, 1–26.

Guidoboni, E., Comastri, A. & Traina, G. (1994). *Catalogue of Ancient Earthquakes in the Mediterranean Area up to the 10th Century*. ING-SGA, Bologna, p. 504

Guidoboni, E. & Comastri, A. (2005)a. *Catalogue of Earthquakes and Tsunamis in the Mediterranean area From the 11th to the 15th Century*. INGV-SGA, Bologna.

Guidoboni, E. & Comastri, A. (2005)b. Two thousand years of earthquakes and tsunamis in the Aegean are (from 5th BC to 15th century). *International Symposium on the Geodynamics of Eastern Mediterranean: Active Tectonics of the Aegean Region*, Abstract Book: Kadir Has University, 15–18 June, 2005, İstanbul, Turkey, p. 242

Hall, J., Aksu, A.E., Yaltırak, C. & Winsor, J.D. (2008). Structural architecture of the Rhodes Basin: a deep depocentre that evolved since the Pliocene at the junction of Hellenic and Cyprus Arcs, Eastern Mediterranean. *Marine Geology*, doi:10.1016/j.margeo.2008.02.007.

Hancock, P.L., Barka, A.A., (1981). Opposed shear senses inferred from neotectonic mesofractures systems in the North Anatolian fault zone. *J. Struct. Geol.* 3, 383– 392.

Harrison R., Newell W., Panayides I., Stone B., Tsiolakis E., Necdet M., Batihanli H., Ozgur A., Lord A., Berksoy O., Zomeni Z., Schindler J. S. (2008). Bedrock Geologic Map of the Greater Lefkosia Area, Cyprus, USGS.

Jara-Muñoz, J., Melnick D., Strecker M. (2015). Terracem Guide.

Jongsma, D., van Hinte, J.E., Woodside, J.M., 1985. Geological structure and neotectonics of the north African continental margin south of Sicily. *Mar. Pet. Geol.* 2, 156– 179.

Jongsma, D., Woodside, J.M., King, G.C.P., van Hinte, J.E., (1987). The Medina Wrench: a key to the kinematics of the central and eastern Mediterranean over the past 5 Ma. *Earth Planet. Sci. Lett.* 82, 87–106.

Kempler, D. & Garfunkel, Z. (1991). The northeast Mediterranean triple junction from a plate kinematics point of view. *Bulletin of Technical University of İstanbul* 44, 203–232.

Kindler, P., Guillevic, M., Baumgartner, M., Schwander, J., Landais, A., Leuenberger, M., (2014). Temperature reconstruction from 10 to 120 kyr b2k from the NGRIP ice core. *Clim. Environ. Phys.* 10 (2), 887e902.

Kinnaird, T., (2008), Tectonic and sedimentology response to diachronous continental collision in the easternmost Mediterranean, Cyprus, Ph.D. Thesis, University of Edinburgh, Edinburgh, Scotland.

Lajoie, K.R., (1986). Coastal tectonics. In: Wallace, R.E. (Ed.), *Active Tectonics: Impact on Society*. The National Academies Press, Washington, DC, pp. 95e124.

Le Pichon, X., Lyberis, N. & Alvarez, F. (1984). Subsidence history of the North Aegean trough, *Geological Evolution of the Eastern Mediterranean*. Geological Society, London, Special Publications 17, 27–741.

- Lisiecki, L.E., Stern, J.V.**, (2016). Regional and global benthic $\delta^{18}\text{O}$ stacks for the last glacial cycle. *Paleoceanography* 31, 1e27.
- Mascle, J. & Martin, L.** (1990). Shallow structure and recent evolution of the Aegean Sea: a synthesis based on continuous reflection profiles. *Marine Geology* 94, 271–299.
- Mascle, J., Benkhelil, J., Bellaiche, G., Zitter, T., Loncke, Prised II Scientific Party,** (2000). Marine geologic evidence for a Levantine–Sinai plate, a new piece of the Mediterranean puzzle. *Geology* 28, 779– 782
- McCay, G.A., Robertson A.H.F.** (2012). Late Eocene–Neogene sedimentary geology of the Girne (Kyrenia) Range, northern Cyprus: A case history of sedimentation related to progressive and diachronous continental collision.
- Melnick, D., Cisternas, M., Moreno, M., Norambuena, R.**, (2012) a. Estimating coseismic coastal uplift with an intertidal mussel: calibration for the 2010 Maule Chile earthquake (M_w 8.8). *Quat. Sci. Rev.* 42, 29e42.
- Merritts, D., Bull, W.B.**, (1989). Interpreting Quaternary uplift rates at the Mendocino triple junction, northern California, from uplifted marine terraces. *Geology* 17 (11), 1020e1024.
- North Greenland Ice Core Project Members,** (2004). High-resolution record of Northern Hemisphere climate extending into the last interglacial period. *Nature* 431, 147e151.
- Papazachos, B.C., Papaioannou, Ch.A.**, (1999). Lithospheric boundaries and plate motions in the Cyprus area. *Tectonophysics* 308, 193–204.
- Pedoja, K., Ortlieb, L., Dumont, J.F., Lamothe, M., Ghaleb, B., Auclair, M., Labrousse, B.**, (2006). Quaternary coastal uplift along the Talara Arc (Ecuador, Northern Peru) from new marine terrace data. *Mar. Geol.* 228 (1e4), 73e91.
- Pedoja, K., Husson, L., Regard, V., Cobbold, P.R., Ostanciaux, E., Johnson, M.E., Kershaw, S., Saillard, M., Martinod, J., Furgerot, L., Weill, P., Delcaillau, B.**, (2011) a. Relative sea-level fall since the last interglacial stage: Are coasts uplifting worldwide? *Earth Sci. Rev.* 108, 1–15.
- Pedoja, K., Regard, V., Husson, L., Martinod, J., Guillaume, B., Fucks, E., Iglesias, M., Weill, P.**, (2011) b. Uplift of Quaternary shorelines in Eastern Patagonia: Darwin revisited. *Geomorphology* 127 (2011b), 121–142.

Pedoja, K., Husson, L., Johnson, M., Melnick, D., Witt, C., Pochat, S., Nexer, M., Delcaillau, B., Pinegina, T., Poprawski, Y., Authemayou, C., Elliot, M., Regard, V., Garestier, F., (2014). Coastal staircase sequences reflecting sea-level oscillations and tectonic uplift during the Quaternary and Neogene. *Earth Sci. Rev.* 132, 13–38

Philip, H., Cisternas, A. & Gorshkov, A. (1989). The Caucasus: an actual example of the initial stages of continental collision. *Tectonophysics* 161, 1–21.

Poisson, A., Wernli, R., Sağular, E.K. & Temiz, H. (2003). New data concerning the age of the Aksu Thrust in the south of the Aksu valley, Isparta Angle (SW Turkey): consequences for the Antalya Basin and the Eastern Mediterranean. *Geological Journal* 38, 311–327.

Poole, A.J., Robertson, A.H.F., and Shimmield, G., (1990), Late Quaternary uplift of the Troodos ophiolite, Cyprus; Uranium-series dating of Pleistocene coral, *Geology* 18: pp. 894-897

Robertson, A.H.F., (1998). Tectonic significance of the Eratosthenes Seamount: a continental fragment in the process of collision with a subduction zone in the eastern Mediterranean (Ocean Drilling Program Leg 160). *Tectonophysics* 298, 63– 82.

Rohling, E.J., Marinoa, G., Grant, K.M., (2015). Mediterranean climate and oceanography, and the periodic development of anoxic events (sapropels). *Earth Sci. Rev.* 143, 62e97.

Salamon, A., Hoffstetter, A., Garfunkel, Z. & Ron, H. (1996). Seismicity of the eastern Mediterranean region: perspective from the Sinai subplate. *Tectonophysics* 263, 293–305.

Schattner, U. & Ben-Avraham, Z. (2007). Transform margin of the northern Levant, eastern Mediterranean: from formation to reactivation. *Tectonics* 26, doi:10.1029/2007 TC002112.

Schattner, U., Ben-Avraham, Z., Lazar, M. & Hübischer, C. (2006) a. Tectonic isolation of the Levant basin offshore GalileeLebanon e effects of the Dead Sea fault plate boundary on the Levant continental margin, eastern Mediterranean. *Journal of Structural Geology* 28, 2049–2066.

- Schattner, U., Ben-Avraham, Z., Reshef, M., Bar-Am, G. & Lzar, M.** (2006) b. Oligocene–Miocene formation of the Haifa basin: Qishon–Sirhan rifting coeval with the Red Sea–Suez rift system. *Tectonophysics* 419, 1–12
- Siddall, M., Chappell, J., Potter, E.-K.,** (2006). Eustatic Sea level during past interglacials. In: Sirocko, F., Litt, T., Claussen, M., Sanchez-Goni, M.-F. (Eds.), *The Climate of Past Interglacials*. Elsevier, Amsterdam.
- Şaroğlu, F., Emre, Ö. & Kuşçu, İ.** (1992). *Active Fault Map of Turkey*, 2 Sheets, MTA, Ankara, Turkey
- Şengör, A.M.C., Yılmaz, Y.,** (1981). Tethyan evolution of Turkey: a plate tectonic approach. *Tectonophysics* 75, 181–241.
- Taymaz, T., Jackson, J. & Westaway, R.** (1990). Earthquake mechanisms in the Hellenic Trench near Crete. *Geophysical Journal International* 102, 695–731.
- Taymaz, T., Jackson, J.A. & Mckenzie, D.** (1991). Active tectonics of the north and central Aegean Sea. *Geophysical Journal International* 106, 433–490.
- Taymaz, T., Westaway, R. & Reilinger, R.** (2004). Active faulting and crustal deformation in the Eastern Mediterranean Region. *Tectonophysics* 391, 1–9.
- Taymaz, T., Yılmaz, Y. & Dilek, Y.** (2007) a. Introduction. In: Taymaz, T., Yılmaz, Y. & Dilek, Y. (eds), *The Geodynamics of the Aegean and Anatolia*. Geological Society, London, Special Publications 291, 1–16
- Tsiolakis, E., Zomeni, Z.,** (2008), Geological map of the Pafos – Kallepeia area, Sheets 16 III & IV, scale 1:25,000, Cyprus Geological Survey
- Waelbroeck, C., Labeyrie, L., Michel, E., Duplessy, J.C., Lambeck, K., McManus, J.F., Balbon, E., Labracherie, M.,** (2002). Sea-level and deep water temperature changes derived from benthic foraminifera isotopic records. *Quat. Sci. Rev.* 21, 295e305.
- Woodside, J., Mascle, J. Huguen, C. & Volkonskaia, A.** (2000). The Rhodes Basin, a Post-Miocene tectonic trough. *Marine Geology* 165, 1–12.
- Woodside, J.M., Mascle, J., Zitter, T. A.C., Limonov, A. F., Ergun, M. & Volkonskaia, A.** and a shipboard scientists of the PRISMED II expedition

(2002). The Florence Rise, the western bend of the Cyprus Arc. *Marine Geology* 185, 177–194

Veen, J.H., Woodside J.M., Zitter, T. A.C., Dumont, J.F., Mascle, C., Volkonskaia, A., (2004). Neotectonic evolution of the Anaximander Mountains at the junction of the Hellenic and Cyprus arcs. *Tectonophysics* 391, 35– 65.

Yolsal, S., Taymaz, T. & Yalçiner, A.C. (2007)a. Understanding tsunamis, potential source regions and tsunami prone mechanisms in the Eastern Mediterranean. In: Taymaz, T., Yılmaz, Y. & Dilek, Y. (eds), *The Geodynamics of the Aegean and Anatolia*. Geological Society, London, Special Publications 291, 201–230.

Yolsal, S., Taymaz, T. & Yalçiner, A.C. 2007b. Source characteristics of earthquakes along the Hellenic and Cyprus Arcs and simulation of historical tsunamis, *Geophysical Research Abstracts* 9, European Geosciences Union General Assembly (2007), EGU-2007-A-02306, Vienna, Austria.

Yolsal, S., Taymaz, T. & Yalçiner, A.C. 2008a. Earthquake source rupture characteristics along the Hellenic Arc and simulation of the AD 365 Crete earthquake and its tsunami. *Geophysical Research Abstracts* 10, EGU-2008-A-00065, European Geosciences Union General Assembly (2008), Vienna, Austria.

Yolsal, S., Taymaz, T. & Yalçiner, A.C. 2008b. Source mechanisms of the recent Rhodes-Dodecanese Islands earthquakes and historical tsunami simulations in the eastern Mediterranean. *Geophysical Research Abstracts* 10, EGU-2008-A-00072, European Geosciences Union General Assembly (2008), Vienna, Austria.

Yolsal, S., Taymaz, T. (2009). Sensitivity Analysis on Relations Between Earthquake Source Rupture Parameters and Far-Field Tsunami Waves: Case Studies in the Eastern Mediterranean Region. *Turkish Journal of Earth Sciences (Turkish J. Earth Sci.)*, Vol. 19, 2010, pp. 313–349.

Zanchi, A., Crosta G.B. & Darkal, A.N. (2002). Paleostress analyses in NW Syria: constraints on the Cenozoic evolution of the northwestern margin of the Arabian plate. *Tectonophysics* 357, 255–278

Zitter, T.A.C., Woodside, J.M., Mascle, J., (2003). The Anaximander Mountains: a clue to the tectonics of southwest Anatolia. *Geol. J.* 38, 375–394.

Zomeni Z. (2012). Quaternary Marine Terraces on Cyprus: Constraints on Uplift and Pedogenesis, and the Geoarchaeology of Palaipafos, PhD thesis.



CURRICULUM VITAE



Name Surname : Cevza D. Altınbaş
Place and Date of Birth : İstanbul 1991
E-Mail : cvzltlbs@gmail.com

EDUCATION

- **B.Sc.** : 2015, Istanbul University, Faculty of Engineering, Geophysical Engineering.
- **M.Sc.** : 2018, Istanbul Technical University, Eurasia Institute of Earth Science, Solid Earth Sciences.

PROFESSIONAL EXPERIENCE AND REWARDS:

- 2012-2014 ISTANBUL University at the Assoc. Prof. Yılmaz Ispir Paleomagnetism Laboratory.
- 2014 Geophysical Engineer- SRC Engineering
- 2015 Completed Bachelorate at ISTANBUL University
- 2015-2016 Geophysical Engineer- Tespit Engineering
- 2016-2017 Geophysical Engineer and Chief of Field- Atasan Engineering
- 2018- Assistant of Acquisitions, Sales & Formats in Ay Production Inc.
- 2018 Completed Master at ISTANBUL Technical University

PUBLICATIONS, PRESENTATIONS AND PATENTS ON THE THESIS:

- Yıldırım C.,Tüysüz O, Melnick D., Altınbaş C.D., Öztürk M., Özcan O., Baykara M., Shen C.,69. *Türkiye Jeoloji Kurultayı* Coastal Tectonic Geomorphology Of The Northern Cyprus; Preliminary Results From Marine Terraces, Wave-Cut Notches, Tsunami Deposits, Off-And Onshore Surface Ruptures.

- Yıldırım C.,Tüysüz O, Melnick D., Altınbaş C.D., Öztürk M., Özcan O., Baykara M., Shen C., *TURQUA VII. Türkiye Kuvaterner Sempozyumu, İstanbul Teknik Üniversitesi Avrasya Yer Bilimleri Enstitüsü 8-11 Mayıs 2016*, Preliminary Results Of The Pleistocene And Holocene Tectonic Deformations Along The Northern Cyprus Coast.
- Altınbaş C.D., *EGU 2016 Vienna* Distribution of Deformation on Cyprus, Inferences from Morphotectonic Analysis.
- Sondaja Dayalı Zemin ve Temel Etüt Çalışması: İstanbul-Ataşehir Örneği” *Graduation Thesis-2014*.

